

Sedimentology and Paleoenvironment of an Early Jurassic Dinosaur Bone Bed, Wasson

Bluff, Parrsboro, Nova Scotia

Leigh van Drecht

Submitted in Partial Fulfillment of the Requirements

For the Degree of Bachelor of Sciences, Honours

Department of Earth Sciences

Dalhousie University, Halifax, Nova Scotia

March 2014

Distribution License

DalSpace requires agreement to this non-exclusive distribution license before your item can appear on DalSpace.

NON-EXCLUSIVE DISTRIBUTION LICENSE

You (the author(s) or copyright owner) grant to Dalhousie University the non-exclusive right to reproduce and distribute your submission worldwide in any medium.

You agree that Dalhousie University may, without changing the content, reformat the submission for the purpose of preservation.

You also agree that Dalhousie University may keep more than one copy of this submission for purposes of security, back-up and preservation.

You agree that the submission is your original work, and that you have the right to grant the rights contained in this license. You also agree that your submission does not, to the best of your knowledge, infringe upon anyone's copyright.

If the submission contains material for which you do not hold copyright, you agree that you have obtained the unrestricted permission of the copyright owner to grant Dalhousie University the rights required by this license, and that such third-party owned material is clearly identified and acknowledged within the text or content of the submission.

If the submission is based upon work that has been sponsored or supported by an agency or organization other than Dalhousie University, you assert that you have fulfilled any right of review or other obligations required by such contract or agreement.

Dalhousie University will clearly identify your name(s) as the author(s) or owner(s) of the submission, and will not make any alteration to the content of the files that you have submitted.

If you have questions regarding this license please contact the repository manager at dalspace@dal.ca.

Grant the distribution license by signing and dating below.

Name of signatory

Date



**DALHOUSIE
UNIVERSITY**

Inspiring Minds

Department of Earth Sciences

Halifax, Nova Scotia

Canada B3H 4R2

(902) 494-2358

FAX (902) 494-6889

DATE: April 22, 2014

AUTHOR: Leigh van Drecht

TITLE: Sedimentology and Paleoenvironment of an Early
Jurassic Dinosaur Bone Bed, Wasson Bluff, Parrsboro,
Nova Scotia

Degree: B.Sc. Hons Convocation: May Year: 2014

Permission is herewith granted to Dalhousie University to circulate and to have copied for non-commercial purposes, at its discretion, the above title upon the request of individuals or institutions.

Leigh van Drecht
Signature of Author

THE AUTHOR RESERVES OTHER PUBLICATION RIGHTS, AND NEITHER THE THESIS NOR EXTENSIVE EXTRACTS FROM IT MAY BE PRINTED OR OTHERWISE REPRODUCED WITHOUT THE AUTHOR'S WRITTEN PERMISSION.

THE AUTHOR ATTESTS THAT PERMISSION HAS BEEN OBTAINED FOR THE USE OF ANY COPYRIGHTED MATERIAL APPEARING IN THIS THESIS (OTHER THAN BRIEF EXCERPTS REQUIRING ONLY PROPER ACKNOWLEDGEMENT IN SCHOLARLY WRITING) AND THAT ALL SUCH USE IS CLEARLY ACKNOWLEDGED.

Abstract

The Early Jurassic McCoy Brook Formation at Wasson Bluff on the northern side of the Minas subbasin has been a site of dinosaur bone discoveries for over thirty years. Excavations at the Princeton Quarry in 1998-2006 recovered at least three articulated prosauropods within a confined bone bed. This bone bed includes the oldest dinosaur bones in Canada and richest prosauropod site in North America. The dinosaur material has been well documented but the detailed sedimentology of the bone-bearing bed is of interest for analyzing the paleoenvironment and taphonomy of the prosauropods.

A five-meter section that includes the bone-bed and overlying units was described at a centimeter scale over the course of 10 days of field work during the 2013 excavation. Representative samples of the strata were collected for grain-size and petrologic analysis.

Laser diffraction grain-size analysis, shows that poorly sorted, fine- to medium grained sandstone predominates. Scatter plots with combinations of skewness, mean and sorting allowed separation of facies and support the identification of two facies associations. In the lower part of the section, interbedded thin, red, micaceous mudstone and orange-brown sandstone show cross-beds and ripple lamination. These strata are attributed to fluvial deposition. In the upper part of the section, large cross-sets of grey-brown sandstone with light and dark laminae predominate, and the sandstones are coarser and better sorted than those below. These strata are attributed to eolian deposition. Outsized, moderately rounded grains in the fluvial sandstones suggest eolian additions.

Sandstones are immature and were classified as feldspathic litharenite and lithic arkose. During diagenesis they were minimally compacted with a clay matrix and cementation by gypsum to form small nodules. Grains are coated by hematite and clay giving the sandstones a characteristic red-bed appearance.

Prosauropod bones were found in two beds of trough cross-bedded sandstone in the lower part of the section and were in some cases crushed by compaction of sandstones as a result of minimal permineralization of the bones as well as being offset by small centimeter-scale faults. Isolated basalt boulders eroded from an 8 m paleocliff face nearby were deposited in bone-bearing beds but also occur in units that do not contain bones.

Detailed sedimentological analysis provides new information that is useful for interpreting the depositional environment of the bone bed. The results indicate that the dinosaurs were preserved in a fluvial system with episodic flow and periodic desiccation in a dune field filling a micro-basin. Dinosaurs may have been overwhelmed by flooding in a narrow basin and/or a moderate flow may have concentrated the bloated carcasses.

Keywords: Prosauropod, McCoy Brook Formation, Princeton Quarry, taphonomy, micro-basin, eolian-fluvial interaction.

Table of Contents

Abstract	I
Table of Figures	IV
List of Tables	V
Acknowledgements	VI
Chapter 1: Introduction	1
1.1 The Wasson Bluff Dinosaur Site	1
1.2 Excavation in 2013	2
Chapter 2: Regional Geology	5
2.1 The Break-up of Pangea	5
2.2 Fundy Rift Complex, Minas Subbasin & Fundy Group Formations	5
2.3 McCoy Brook Formation	9
2.3.1 Type Section	10
2.3.2 Wasson Bluff	11
2.3.3 McCoy Brook Formation Preservations	11
2.3.4 Princeton Quarry	13
Chapter 3: Methodology	17
3.1 Field Analysis	17
3.1.1 Megascopic Observations	17
3.1.2 Microscopic Observations	17
3.2 Grain-size Analysis	18
3.2.1 Laser Diffraction	18
3.2.2 Preparing Samples and Analysis	20
3.2.3 Interpreting Grain Size	21
Chapter 4: Lithological Observation and Description	22
4.1 Stratigraphic Section	22
4.2 Facies 1: Red-brown mudstone	22
4.3 Facies 2: Orange-brown sandstone	26
4.4 Facies 3: Light grey-brown sandstone	28
4.5 Facies Associations	29

4.6 Basalt Boulders	30
Chapter 5: Grain Size Analysis and Petrography	32
5.1 Grain Size Analysis	32
5.1.1 Introduction	32
5.1.2 Mean and Distribution	32
5.1.3 Modes.....	34
5.1.4 Skewness and Sorting	35
5.2 Petrographic Analysis.....	40
Chapter 6: Discussion	46
6.1 Interpretations	46
6.1.1 Facies Association 1	46
6.1.2 Facies Association 2	47
6.1.3 Early Burial History	48
6.1.4 Grain Size Analysis	48
6.1.5 Gypsum Nodules, Iron Oxidation and Mottling	49
6.1.6 Provenance	50
6.1.7 Basalt Boulders.....	51
6.1.8 Paleoenvironment	52
6.2 Taphonomy	55
6.3 Analogues	58
6.3.1 Barun Goyot Formation, Mongolia.....	58
6.3.2 Kayenta and Navajo Formations, Northern Arizona	60
6.3.3 Modern Analogue.....	63
6.4 Future Work	64
Chapter 7: Conclusions.....	66
Appendix A: Summary of lithological observation by bed.	67
Appendix B: Summary of grain size analysis by bed.	68
References	69

Table of Figures

Figure 1.1 Excavation site in 2013 with plastic bags protecting exposed bones.....	3
Figure 1.2 Bone map skewed on the 2013 excavation site.....	3
Figure 2.1 Reconstruction of the continental plates in the Early and Late Jurassic.	7
Figure 2.2 Regional geology of the Fundy Rift Basin and the Minas subbasin.....	8
Figure 2.3 McCoy Brook Formation cropping out at Wasson Bluff.....	11
Figure 2.4 Reconstruction of <i>Plateosaurus</i> sp. at the Fundy Geological Museum.....	15
Figure 3.1 Scattering angles produced by large and small grains	19
Figure 3.2 Fourier lens used in laser diffraction.....	19
Figure 4.1 The measured section, not annotated and annotated.....	24
Figure 4.2 Princeton Quarry stratigraphic column.....	25
Figure 4.3 Sedimentary features of the measured section	27
Figure 4.4 Cross-beds from bed 21and 22, Facies 3.....	28
Figure 4.5 Erosional surfaces and lamination within bed 21, Facies 3.....	28
Figure 5.1 Bar graph showing the distribution of sand, silt and clay	33
Figure 5.2 Ternary diagram showing distribution of sand, silt and clay.....	34
Figure 5.3 Histograms showing grain-size distribution	37
Figure 5.4 Scatter plot showing the relationship between sorting and skewness.....	39
Figure 5.5 Scatter plot showing the relationship between mean and skewness	39
Figure 5.6 Scatter plot showing the relationship between mean and sorting	40
Figure 5.7 Friedman’s boundaries of modern river and dune sand.....	40
Figure 5.8 Sandstone classification of Folk.....	43
Figure 5.9 Examples of facies and detrital grains.....	44
Figure 5.10 Examples of detrital and lithic grains	45
Figure 6.1. Wasson Bluff annotated with facies interpretation	54
Figure 6.2 Painting by Judi Pennanen depicting prosauropods at Wasson Bluff.....	54
Figure 6.3 Large sauropod producing localized pits to entomb small theropods.....	57
Figure 6.4 Stratigraphic column of the Lower Jurassic Glen Canyon Group.....	62
Figure 6.5 Dune field in Western Mongolia to the south of Zavkhan.....	63

List of Tables

Table 2.1 Faunal remains of the McCoy Brook Formation at Wasson Bluff.....	13
Table 2.2 Summary of discoveries at the Princeton Quarry.....	15
Table 5.1 Summary of grain size analysis by facies.....	33
Table 5.2 Summary of detrital minerals and lithic grains in Facies 2 and 3	43
Table 6.1 Summary of taphonomic scenarios for prosauropods at Wasson Bluff.....	57

Acknowledgements

To the faculty and staff in the Earth Sciences Department who made my undergrad so enjoyable and the 2014 honours class who supported and encouraged one another throughout the year. Specifically, Colin Price, with whom many animated discussions took place which often lead far beyond the scope of our projects.

I would like to extend my thanks to Owen Brown at the Bedford Institute of Oceanography and Randolph Corney for the use of their labs as well as their expertise and enthusiasm. Also to Gordon Brown for his help with thin sections.

Finally, thank you to my incredible supervisors, Dr. Martin Gibling and Dr. Tim Fedak for providing me with such a great project. Their wisdom, guidance, and support made the anticipated daunting process of writing a thesis an enjoyable one.

Chapter 1: Introduction

1.1 The Wasson Bluff Dinosaur Site

The Early Jurassic McCoy Brook Formation at Wasson Bluff, on the north side of the Minas subbasin, Nova Scotia, has been a site of active excavations yielding prosauropod bone discoveries for over thirty years (Tanner, 1996). Dinosaur bones have been collected from the Wasson Bluff site since 1976 (Olsen et al., 2005), up to the most recent excavation in August, 2013. The dinosaur material has been well documented and the detailed sedimentology of the bone-bearing bed is of interest for analyzing the taphonomy and paleoenvironment.

The Minas subbasin, one of three basins that comprise the Fundy Rift Basin complex (Tanner, 1996), formed during the break up of Pangea, ~40 Ma prior to the opening of the Atlantic Ocean (Olsen et al., 2005). During the Late Triassic and Early Jurassic, terrestrial sediments eroded from the highlands filled the basin (Tanner and Hubert, 1991). The McCoy Brook Formation crops out along the northern shore of the Minas subbasin where it onlaps the underlying North Mountain Basalt (Tanner, 1996), which in turn rests on the Blomidon Formation. The Blomidon Formation may contain the Triassic-Jurassic boundary determined using palynology (Olsen, 1988) but the position of the boundary is in doubt and has been disputed. The Triassic-Jurassic boundary marks a mass extinction event, and the stratal succession near Parrsboro may provide a unique look at the animals that survived this dramatic time in Earth's history (Olsen et al., 2005).

The first fossil bones were collected from the cliff section in 1976 when Paul E. Olsen and his team from Princeton University (Olsen et al., 2005) located considerable

disarticulated dinosaur material. After the initial discovery, bone material and fragments were found by numerous researchers. Ken Adams and George Hrynewich located the first articulated, almost complete specimen (Fedak, 2006). Since then, five prosauropods have been discovered, three of which are in contact and overlapping, making this site the richest prosauropod site in North America, which contains the oldest dinosaurs in Canada (Olsen et al., 2005). The site was dubbed the Princeton Quarry and is referred to as Site N in publications by Olsen.

1.2 Excavation in 2013

The most recent excavation at Wasson Bluff was conducted over a 10-day period in August, 2013. Motivation to return to the site was due to sufficient finds during previous digs conducted by Tim Fedak and his team. The 2013 team consisted of volunteers who had participated in past digs with varied degrees of experience. During the first couple of days the team worked to expose the main bone bed and swept the face of the cliff in search of any bone that may have been exposed since the last dig (2007) due to erosion. An excavator was used to clear away a large amount of beach and erosional debris in order to expose as much of the bone-bearing unit as possible. Shortly after the excavator began clearing debris, the first disarticulated bone was uncovered. All material found during the 2013 dig was disarticulated bone located to the east of the main localized bone bed (Fig. 1.1). A film crew joined the dig during the last four days to document progress made by the field crew and volunteers for a documentary featuring prominent dinosaur discoveries from across Canada. Local reporters also frequented the dig site as collected specimens from the site are featured in the Fundy Geologic Museum and draw a considerable amount



Figure 1.1 East-facing view of the excavation site showing plastic bags that covered and protected exposed bone during the 2013 excavation. The grey crate is approximately 30 cm.



Figure 1.2 Bone map produced by Fedak (2006) which depicts three prosauropods from the Princeton Quarry that were in contact. The bone map has been skewed to show original position of bones and placed on the excavation site for reference to previous excavation sites. Bones found in 2013 are an eastern extension of this main bone bed.

of local attraction and interest.

During prior excavations of the Princeton Quarry, a field map was produced of the three prosauropods in contact, to document the spatial relationship between sediment and bone (Fedak, 2006) (Fig. 1.2). The field map includes faults, due to their interaction with the fossilized material and provides a sense of displacement. Work at this site has been focused around discovery of new bone and documentation of existing bone. The detailed sedimentology has not been of focus, but the bone map preserves the spatial context.

The purpose of this study is to document a comprehensive account of the strata at the Princeton Quarry and describe the sediment and sedimentary structures at a centimeter scale, beginning at the bone bed. Examining the sedimentological context and depositional structures contributes to the interpretation of the paleoenvironment and taphonomy. Extensive faulting and tectonic activity that occurred during and after sediment deposition adds complexity to the stratigraphy, which limits interpretations.

Chapter 2: Regional Geology

2.1 The Break-up of Pangea

As the African and North American plates separated, the eastern coast of North America was left with a series of failed rifts, marking the breakup of super continent Pangea (van Houten, 1977). One rift, however did not fail and by the Late Jurassic the Atlantic Ocean was beginning to form (Fig. 2.1). One of the failed rifts formed the Fundy Rift Complex, which developed during an arid, hot-house climate (Frakes, 1979) and was at 26° N paleolatitude at the end of the Triassic (Kent and Tauxe, 2005).

2.2 Fundy Rift Complex, Minas Subbasin and Fundy Group Formations

The Fundy Rift Complex is the northernmost and best exposed (Kent and Olsen, 2000) early Mesozoic rift basin to form during the separation of Africa and North America (Schlische and Ackerman, 1995). It is made up of three subbasins (Tanner, 1996) that display two differing structural styles (Olsen et al, 1990), the extensional Fundy and Chignecto subbasins and the transtensional Minas subbasin (Fig. 2.2 A). During extension, the Fundy and Chignecto subbasins formed as NW-tilted half-grabens (Schlische, 1990) and the Minas subbasin was formed through transtensional rifting as a result of the Minas fault zone reactivating as a sinistral strike-slip fault (Olsen and Schlische, 1990). The Minas fault zone had originally been a dextral strike-slip fault during the Carboniferous and marks the boundary between the Avalon and Meguma Terranes (Keppie, 1982).

Terrestrial sediments from the Cobequid Highlands filled the Minas Basin during the Triassic and Jurassic (Tanner and Hubert, 1991) and are known as the Fundy Group (Tanner, 1996). The Fundy Group includes the Late Triassic Wolfville Formation, which lies

unconformably on top of Paleozoic basement (Tanner et al., 1991) and is characterized by fluvial, alluvial-fan and eolian deposits (Hubert et al., 1988). The Late Triassic-Early Jurassic (age in dispute) Blomidon Formation, stratigraphically above the Wolfville Formation, is mostly cyclical lacustrine strata (Kent and Olsen, 2000) and underlies the Early Jurassic (202 ± 2 Ma) North Mountain Basalt (Hodych et al., 1992). The Triassic-Jurassic boundary has been previously identified by the disappearance of Triassic palynomorph *Patinasporites densus* in the uppermost Blomidon Formation (Fowell and Olsen, 1993) but this marker for the boundary has been disputed by Cirilli et al. (2009). Cirilli et al. (2009) suggest that the Triassic-Jurassic boundary lies above or is contemporaneous with the eruption and emplacement of the North Mountain Basalt (part of the Central Atlantic Magmatic Province volcanism, or CAMP), which may have sparked the mass extinction event (Cirilli et al., 2009). Olsen et al (2012) also suggests a bolide impact as a trigger of the mass extinction event using an iridium anomaly that is associated with a fern spike as evidence.

If the Triassic-Jurassic boundary is in fact within or above the North Mountain Basalt, the disappearance of *P. densus* may only reflect a late Triassic magnetic reversal (Cirilli et al, 2009). Blackburn et al (2013) propose that there may have been four discrete pulses of the CAMP eruptions, which are seen in Morocco (Argana Basin), Canada (Fundy Basin) and the United States of America (Newark Basin). Based on relative chronology, the Tasquint Basalt of the Argana Basin is the oldest CAMP unit, the North Mountain Basalt of the Fundy Basin is slightly younger, and the Orange Mountain Basalt of the Newark Basin is younger still (Blackburn et al., 2013).

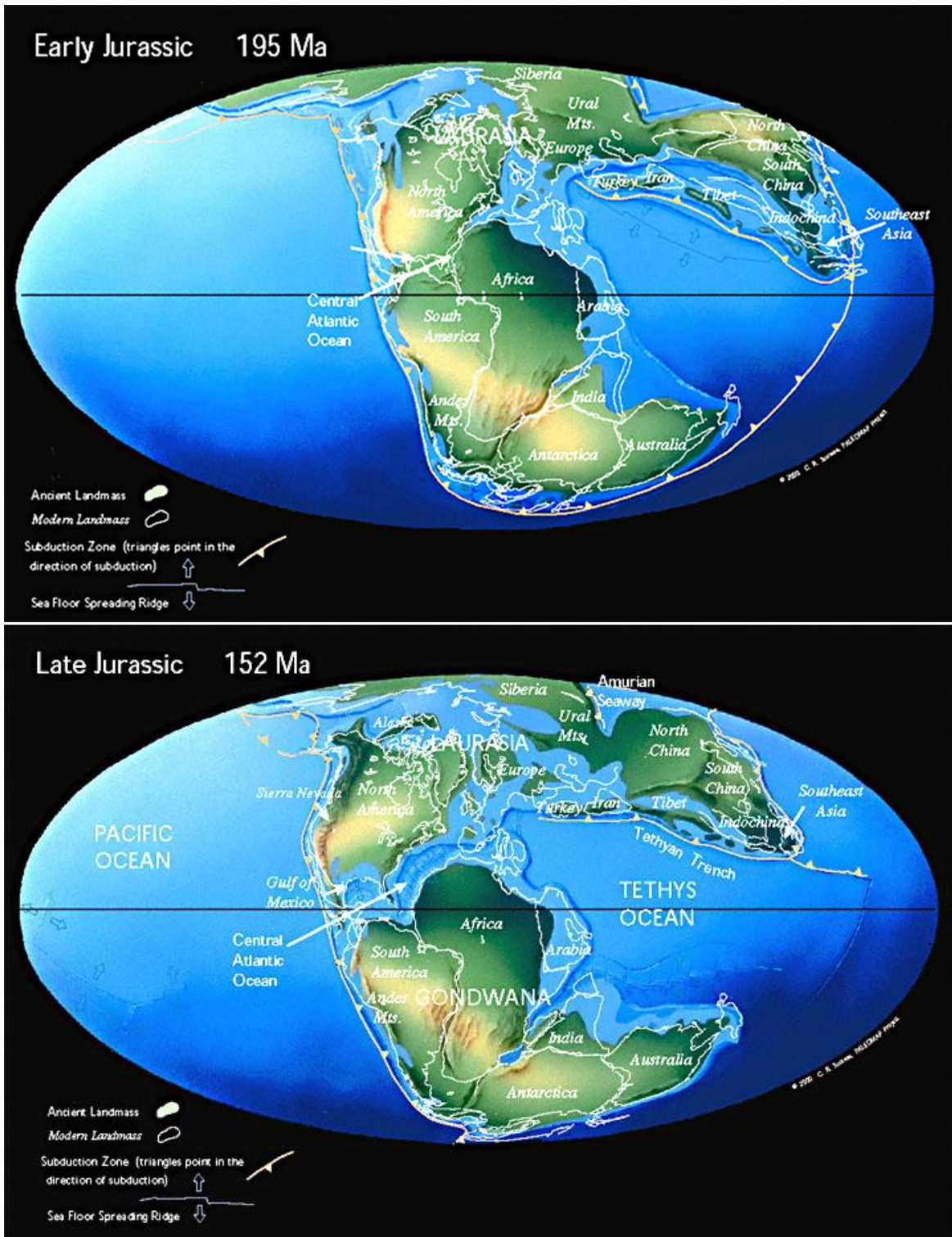
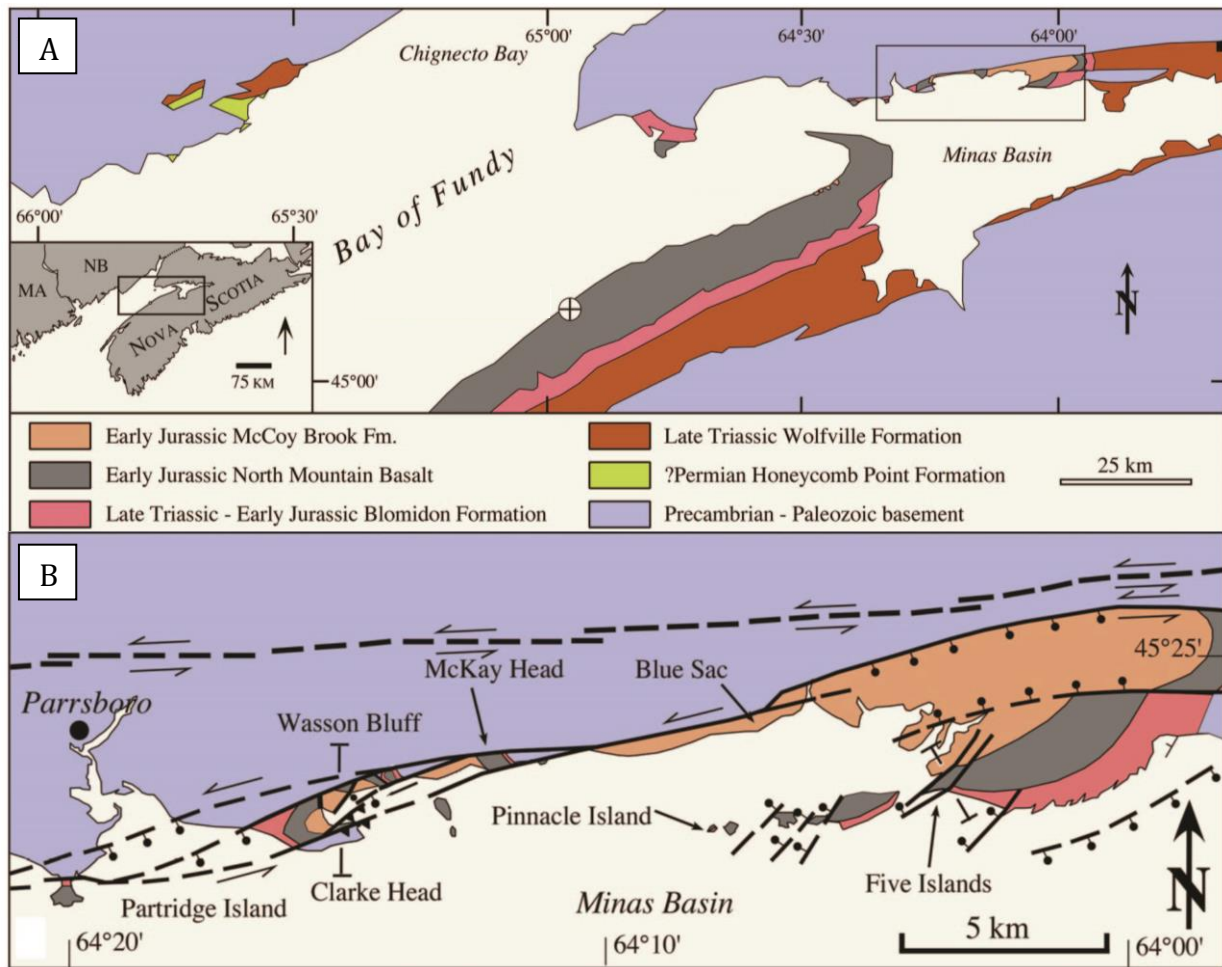


Figure 2.1 Reconstruction of the continental plates in the Early and Late Jurassic (Scotese, 2001).



If the end Triassic extinction was brought on by the eruption of CAMP, the extinction event might logically be placed at the base of the Tasguint Basalt (Morocco) (Blackburn et al., 2013). This would explain why CAMP basalts in the Fundy and Newark Basin appear to post-date the mass extinction event. Using Blackburn's model it would appear that the disappearance of *P. densus* in the Fundy Basin does represent the Triassic-Jurassic boundary and reflects the first pulse of CAMP basalt in Morocco rather than an end-Triassic magnetic reversal as suggested by Cirilli et al. (2009). Considering again the four pulses of

the CAMP basalts, the boundary could be placed at the end of the last pulse. This pulse would mark the end of the eruptions and the end of the extinction event.

The youngest of the Fundy Group is the McCoy Brook Formation, which is the focus of this study and is made up of fluvial, deltaic, lacustrine and eolian strata (Schlische et al., 1995), of Early Jurassic age. Although the position of the Triassic-Jurassic boundary is disputed, an Early Jurassic age for the Princeton Quarry fauna is supported by a lack of dominant Triassic families and abundant vertebrate remains including prosauropod dinosaurs, semionotid and refieldiid fish, *Protosuchus*, *Celvosaurus* and synapsid reptiles (Olsen et al., 1989).

The McCoy Brook Formation can be correlated with formations within the Newark Supergroup including: the Midland Formation of the Culpeper basin, the Feltville Formation of the Newark basin, and the Shuttle Meadow Formation of the Hartford basin. All of these are stratigraphically above the Orange Mountain Basalt, which has a geochemical similarity to the North Mountain Basalt (Olsen et al., 1989).

2.3 McCoy Brook Formation

The McCoy Brook Formation is a syn-tectonic suite of strata (Olsen, 2005) which infilled graben and half-graben micro basins that formed on the surface of the North Mountain Basalt (Tanner, 1996; Olsen and Schlische, 1990). The McCoy Brook Formation consists predominantly of redbeds, basalt conglomerates and basalt breccias (Tanner and Hubert, 1991). Basalt conglomerates and breccias were formed as talus deposits and debris flows which were activated by the steep slopes associated with syndepositional faulting, which occurred during the deposition of the McCoy Brook Formation (Tanner and Hubert,

1991). On the north shore of the Minas subbasin, the redbeds are sandstones and mudstones (Hubert and Mertz, 1984) deposited in lacustrine, fluvial, playa, sandflat, eolian, and alluvial-fan settings (Tanner and Hubert, 1988, 1991). At the base of the McCoy Brook Formation is the Scots Bay Member, which is characterized by lacustrine strata with abundant fish remains (Tanner, 1996). The lake that deposited these strata formed on the undulating surface of the North Mountain Basalt and was big enough to support large aquatic animals (hybodont shark tooth recovered) and to produce wave erosion supported by basalt sandstone present in these strata (Olsen, 1988; Tanner, 1996). On the south shore, the Scots Bay Member of the McCoy Brook Formation crops out as limestones, mudstones, cherts, and sandstones (Tanner, 1996).

2.3.1 Type Section

The type section of the McCoy Brook Formation is named after McCoy Brook, which drains into the Minas Basin 400 m west of McKay Head (Tanner, 1996). As described by Tanner (1996), this section is dominated by 20-30° west-dipping interbedded mudstone and sandstone, fissile claystone and horizontally laminated to ripple cross-laminated sandstone. Muddy sandstone beds have thicknesses ranging from 3 to 50 cm and sandy mudstone beds from 1 to 50 cm. Muddy sandstones and sandy mudstones are massive to finely laminated with sandstones displaying ripple cross-lamination and mudstones displaying desiccation cracks (Tanner, 1996). Gypsum nodules occur only at the top of the section. This section was interpreted to be a playa mudflat deposited on a valley floor with alluvial-fan lobes prograding over the playa lakes to deposit laminated sand and mud packages (Tanner, 1996).



Figure 2.3 North Facing photo of Wasson Bluff. North Mountain Basalt on the west side is faulted against McCoy Brook Formation and forms a paleocliff that resulted from the formation of a half-graben.

2.3.2 Wasson Bluff

At Wasson Bluff two microbasins (Fig. 2.2b) are exposed along cliffs eroded by waves and tides. The western microbasin (Fig 2.3) is a 450 m wide, tilted half graben (Olsen et al., 1989) primarily filled with, west-dipping (tectonically controlled) eolian McCoy Brook strata. Approximately 48 m of dune sand, which is thickened by faulting, fills this basin yielding a paleo-wind direction of 241° (Hubert and Mertz, 1984). On the eastern border of the microbasin, lacustrine strata dubbed the “fish bed”, onlaps the North Mountain Basalt. Approximately 53 m (Fedak, 2007) up-section from the fish bed is the location of the Princeton Quarry, which is the focus of this study.

The basin is bordered on the west by an 8 m high (Hubert and Mertz, 1984) paleo-cliff (Fig. 2.3) of North Mountain Basalt formed by the footwall of the half-graben. This paleo-cliff has eroded, producing basalt boulders that are incorporated into the McCoy Brook Formation as it was being deposited. The boulders appear to be present on first-order surfaces of eolian dunes (Hubert and Mertz, 1984) and boulders become more abundant up-section to the west. Strata at the Princeton Quarry are west-northwest striking ($285-315$) and dips from 25° to 35° (Fedak, 2006).

2.3.3 McCoy Brook Formation Preservations

Olsen (1989) divided the McCoy Brook Formation into five facies rich in fossil material and each with a prevailing suite of taxa (Table 2.1). The following summary of taxa is based on Olsen (1989). The five facies are limestones and siltstones of the fish bed, talus slope breccia, lake margin sandstones, playa sandstone and eolian sandstones.

The fish bed facies is dominated by *Semionotus*, the teeth of *Hybodus* sp., and scales from an undetermined redfieldiid palaeonisciform. Other fossils in this facies include ornithischian dinosaur bones and teeth, protosuchid remains and teeth possibly from a theropod dinosaur (Olsen et al., 1989).

Due to the clast supported nature of the talus-slope breccia facies, small animals were able to live in the spaces between clasts, allowing this facies to yield the most abundant bone remains. Talus slope breccias are dominated by *Protosuchus*, *Hemiprotosuchus* and *Pachygenelus* sp.. Disarticulated and articulated material is present but many of the bones have been truncated by intensive faulting.

Lake-margin sandstone and associated fluvial sandstones are dominated by protosuchid crocodylians along with sphenodontid and *Pachygenelus* sp.. Playa sandstones house some of the most poorly preserved fossils which is dominated by ichnotaxa of *Grallator* (*Anchisauripus*) cf. *sillimani* and *Batrachopus* sp..

The fifth facies, eolian sandstone, is the facies that is the focus of this study. This facies is the site of the first prosauropod discovery at the Princeton Quarry. All of the vertebrates present in the McCoy Brook Formation were present in the Late Triassic but, due to the absence of the dominant Late Triassic families, the McCoy Brook Formation at the level of the Princeton Quarry appears to be Early Jurassic and represent the survivors of the Triassic-Jurassic extinction (Olsen et al., 1989).

2.3.4 Princeton Quarry

Prosauropods lived from the Late Triassic to the Middle Jurassic, were widely distributed and have been found on every continent (Sereno, 1997). Prosauropods (Fig. 2.4) were herbivorous nonobligatory biped dinosaurs with a delicate, small skull relative to their body size (Sereno, 1997). Teeth of this clade do not appear to be efficient at processing plant matter, unlike later sauropods, making gastroliths an important feature for processing food in the gut.

Prosauropods have been identified as a monophyletic group by Sereno (1986) due to hand characteristics, especially the thumb, although more recent studies suggest that prosauropod taxa are likely a paraphyletic assemblage with respect to sauropoda and are now often referred to as basal sauropodomorphs (Yates et al., 2009). The understanding of sauropodomorph phylogenetics is continually developing and for this study, the term

Table 2.1 Summary of faunal remains of the McCoy Brook Formation at Wasson Bluff. Table is modified from Olsen et al 1989.

	Taxa
Talus slope deposits	protosuchid crocodyliform <i>Protosuchus micmac</i>
	trithelodont synapsid, <i>Pachygenelus cf monus</i>
	sphenodontian <i>Clevosaurus bairdi</i>
	ornithischian dinosaurs resembling <i>Lesothosaurus</i>
	probable theropod
Scots Bay Member	Semionotus sp.
	<i>Hybodus</i> teeth and spines
	redfieldiid fish
	tetrapod
	protosuchid crocodyliform <i>Protosuchus micmac</i>
	theropod dinosaur tetth similar to <i>Syntarsus</i>
	ornithischian dinosaur
	<i>Cleavosaurus bairdi</i>
<i>Pachygenelus cf. monus</i>	
Eolian and Fluvial Sandstones	Prosauropod

prosauropod will be used to maintain continuity with previous studies done on this area.

The timeline of prosauropod discoveries at the Princeton Quarry is based on the summary of Olsen et al. (2005). The first prosauropod dinosaur found at Wasson Bluff was located in the center of the western half-graben (Fig. 2.3) on August 7, 1976. Olsen discovered elongate cervical vertebrae of a prosauropod dinosaur while mapping the outcrop. In the following days Olsen and colleagues from Princeton continued to collect prosauropod bones, including a partial femur. This site was dubbed the Princeton Quarry and will be referred to as such throughout this thesis. Originally these first discoveries were thought to be from *Ammosaurus*, a sauropodomorph of the Portland Formation (Early Jurassic) in the Connecticut Valley. Olsen and Gore (1989) documented that these first discoveries were preserved within eolian sandstones but in a subsequent Field Guide Olsen noted:

“... skeletal material is associated with abundant thin micaceous mud-drapes, mud-cracks, ripple surfaces, as well as a thicker (~5cm) layer of fluvial mudstone, suggesting these dinosaurs were preserved in a localized fluvial deposit within an interdune area” (Olsen et al., 2005).

Some years later, Bob Grantham uncovered more bone fragments at the Princeton Quarry. From 1992 to 1994 an almost complete (missing the skull) and articulated sauropodomorph (FGM994GF69) was collected by George Hrynewich and Ken Adams. This specimen is smaller than the original Princeton Quarry specimen (PU22196) discovered by Olsen. The third discovery (FGM998GF9) from the Princeton Quarry was made by Tim

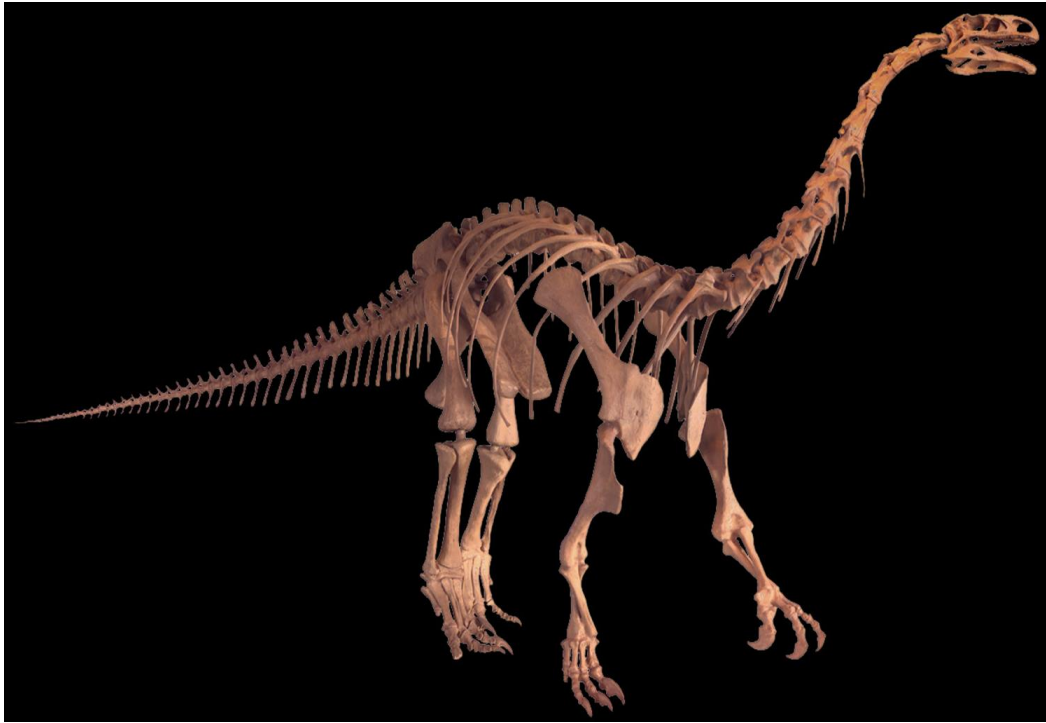


Figure 2.4 Reconstruction of *Plateosaurus* sp. (related prosauropod to those from Wasson Bluff) on display at the Fundy Geological Museum, Parrsboro. (Photo by A. MacRae)

Table 2.2 Summary of discoveries at the Princeton Quarry.

Year	Person	Type of Specimen	Specimen ID
1976	Paul Olsen	disarticulated	PU22196
1992-1994	Discovery: Bob Grantham Collected: George Hrynewich & Ken Adams	articulated	FGM994GF69
1997-2006	Tim Fedak	disarticulated	FGM998GF9
1998-2004	Tim Fedak	articulated	FGM998GF13_I FGM998GF13_II FGM998GF13_III
2013	Tim Fedak	disarticulated	ID unknown

Fedak in 1997. After multiple excavations, many disarticulated bones were collected, including a complete left femur and articulated ischium. Fedak, too, noted that skeletal material was associated with distinctive sedimentary structures including mud beds, ripples, and desiccation cracks attributed to fluvial deposition (Fedak, 2006), and he suggested that specimens were not buried solely in eolian dunes. The following year (1998) another articulated specimen (FGM998GF13_I) was found which led to the discovery of two more specimens (FGM998GF13_II, FGM998GF13_III) in subsequent years. These last three specimens are in contact with one another and overlap making the Princeton Quarry the richest prosauropod bone bed in North America. Similar bone beds include the Wolcott Quarry of the Hartford Basin and Lower Jurassic basal sauropodomorphs from Arizona (Fedak, 2006).

Chapter 3: Methodology

3.1 Field Analysis

The most recent excavation at the Princeton Quarry site was carried out in August 2013. During the course of the field work, samples from a five-meter section of the cliff were collected for grain size and petrological analysis. At the discovery site, the bone map (Fedak, 2006) and bones recovered in 2013 provided a contextual relationship between sediment and bone.

3.1.1 Megascopic Observations

During the course of the field work a stratigraphic section was chosen based on accessibility and deformation due to the severe faulting in the area. A bed-by-bed description included mineralogy, sedimentary structures, bed contacts and other identifying features such as the presence of bone. Using data collected over a 5-meter interval, a stratigraphic column was produced using the drafting software SedLog (Zervas et al, 2009). The column was then re-drafted in Adobe Illustrator to show finer detail and structures such as cross-bedding and ripple lamination. The stratigraphic column was used to document the location and prevalence of facies, which in turn aided in interpreting the environments in which the sediment was deposited.

3.1.2 Microscopic Observations

Microscope observations were made using thin sections cut by Gordon Brown at Dalhousie University. Samples for thin-section analysis were chosen based on their cohesion. For each thin section, mineralogy, grain shape, sorting and cement of the sample was noted. These features were also noted in samples that were not suitable to produce a

thin-section. Grain composition was used to interpret the source of the grains and maturity of the sandstones. Grain shape and sorting give insight into how far individual grains have travelled and by what type of medium they were deposited.

Point counting was carried out at Saint Mary's University using Petrog (Conwy Valley Systems Ltd.), a petrographic data collection program that uses an automated stepping stage. A total of seven slides were analyzed using 400 points per slide. The spacing of the points were adjusted to cover as much of the thin section as possible. After grains are counted, Petrog can produce ternary diagrams with adjustable axes.

3.2 Grain-size Analysis

Grain-size analysis was completed at the Bedford Institute of Oceanography in the Sedimentary Laboratory over a period of five weeks. Quantitative grain-size data provide insight into the mode of transportation and energy of the environment.

3.2.1 Laser Diffraction

Grain size for this study was measured using the Beckman Coulter LS 13 230 laser at the Bedford Institute of Oceanography. The methodology for the use of the laser is based on Beckman Coulter Inc. (2011). The Coulter LS 13 230 uses laser diffraction and light scattering to determine grain size from nanometers to millimeters. This is an absolute method and was chosen because of the wide detectable grain-size range, speed and instant feedback. Laser diffraction has largely replaced the use of sieving and settling tubes to determine grain size because of these multiple advantages.

The LS 13 320 measures the diffraction pattern created by the scattered light caused by the particle or grain. The diffraction pattern is formed by the light intensity due to the

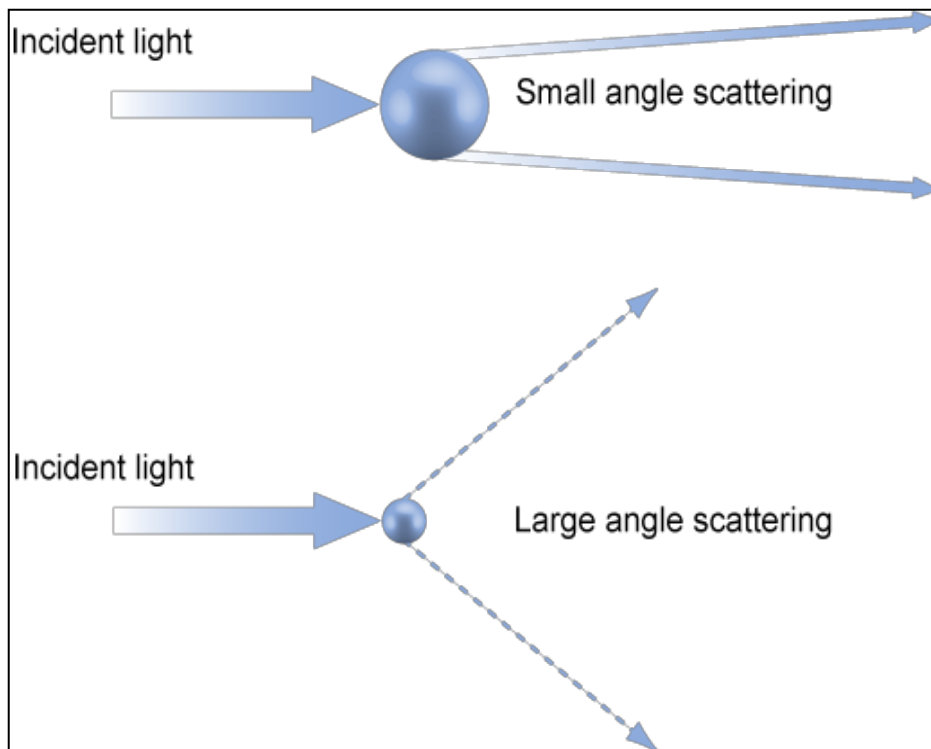


Figure 3.1 Scattering angles produced by large and small grains (Malvern Instruments)

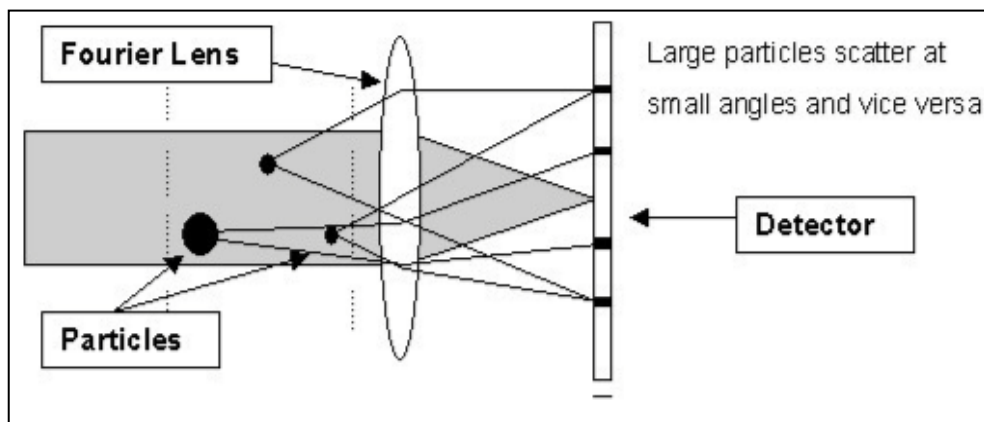


Figure 3.2 Fourier lens focusing and centering diffraction patterns on the detector regardless of grain position (Beckman Coulter Inc, 2011).

scattering angle. This scattering angle is a function of grain size. Large grains have small scattering angle whereas small grains have large scattering angle (Fig. 3.1). This produces a unique diffraction pattern for each grain size. A Fourier lens plays an important part in the function of the LS 13 320 by focusing the scattering light on the detection plane. The Fourier lens (Fig. 3.2) also centers the scattering pattern on the detector, which avoids complications caused by the velocity and location of the grain in the beam of light.

3.2.2 Preparing Samples and Analysis

Preparation of samples for grain-size analysis included disaggregation, weighing, and splitting of the samples to obtain a suitable volume for laser to analyze. Samples were weakly cemented and easily disaggregated with a mortar and pestle. Once disaggregated, samples were transferred to a ceramic dish and placed in an oven (set at 60° C) overnight to draw out all the moisture. Samples were then transferred to plastic vials for storage. The ceramic dishes and plastic vials were weighed with and without the samples to determine sample weight.

The Coulter LS 13 230 can analyze samples with an obscuration between 8 to 12%. Samples were split using a sample splitter until the correct obscuration was obtained. The amount that the sample was split was dependent on the weight of the sample as a whole and the predominant grain size. Finer grained mud samples need about 0.7 g to produce the correct obscuration whereas larger grained sand samples needed about 2 g of sample. When a sample was ready to be analyzed the laser was set on a rinse mode, which lasted approximately two minutes to prepare it for the analyses. The laser was then activated and the sample was placed in the input chamber.

GRADISTAT (Blott and Pye, 2001), a particle size analysis software, uses the raw data produced by Coulter LS 13 230 equipment to generate grain-size distribution graphs. The program calculates mean, standard deviation and skewness in phi unit the using method of moments and the Folk & Ward method. For this study the data generated using the Folk & Ward method were used.

3.2.3 Interpreting Grain Size

To interpret environmental conditions, grain-size data are plotted as grain-size distributions, and scatter plots using combinations of mean, sorting and skewness. Samples from the suite were compared with one another to determine separation of facies and in turn differing depositional processes, perhaps characteristic of certain environments. A useful comparator to consider for this type of study is the boundaries determined by Friedman (1961) which separate modern beach, dune and river sands. Friedman created criteria by plotting different combinations of mean, skewness, kurtosis and standard deviation, identifying fields in which the river, dune and beach sands cluster. Although Friedman's plot is not able to distinguish a depositional environment for the suite of data in this study (all data fall within the overlap area), it provides useful relative trends to consider, such as river sand having a larger standard deviation than dune sand.

Mean, sorting and skewness parameters are used for the comparison of sandstone beds. Sorting cannot be used to compare sandstone to mudstone beds, although it does provide insight into the addition of sand-sized grains in muddy beds and thus insight into depositional conditions.

Chapter 4: Lithological Observation and Description

4.1 Stratigraphic Section

A 567-cm section that includes the bone bed and overlying strata is the focus of this study. This section was chosen due to its continuity and accessibility (Fig. 4.1). It is an area of the cliff that has the least amount of faults and is accessible low in the cliff face. The stratigraphic section was not able to be extended below the bottom-most bed (bone bed) because it is located at beach level. Beds appear to be laterally continuous over a 5-meter traverse of the excavation site with constant thickness although it is difficult to correlate beds across the cliff face due to faulting at varied scales. Contacts of beds are abrupt and linear (Fig. 4.2) with the exception of one contact (bed 4 and 5) that is abrupt and erosional.

Three lithofacies were recognized in this section, distinguished by colour, sedimentary structures and grain-size distributions (Fig. 4.3): red-brown mudstone (Facies 1), orange-brown sandstone (Facies 2) and light grey-brown sandstone (Facies 3).

4.2 Facies 1: Red-brown mudstone

The mudstone facies is red-brown and present mainly as thin interbeds that range from 0.5 – 1 cm in thickness. The facies include beds dominated by clay-size particles and other beds that incorporate fine- to medium grained sand in the mudstone. Generally the finer grained clay and silt beds are present as thin interbeds, whereas thicker beds tend to

incorporate more fine-grained sand. Facies 1 beds are weakly to moderately stratified and contain moderate amounts of mica grains concentrated on laminar surfaces.

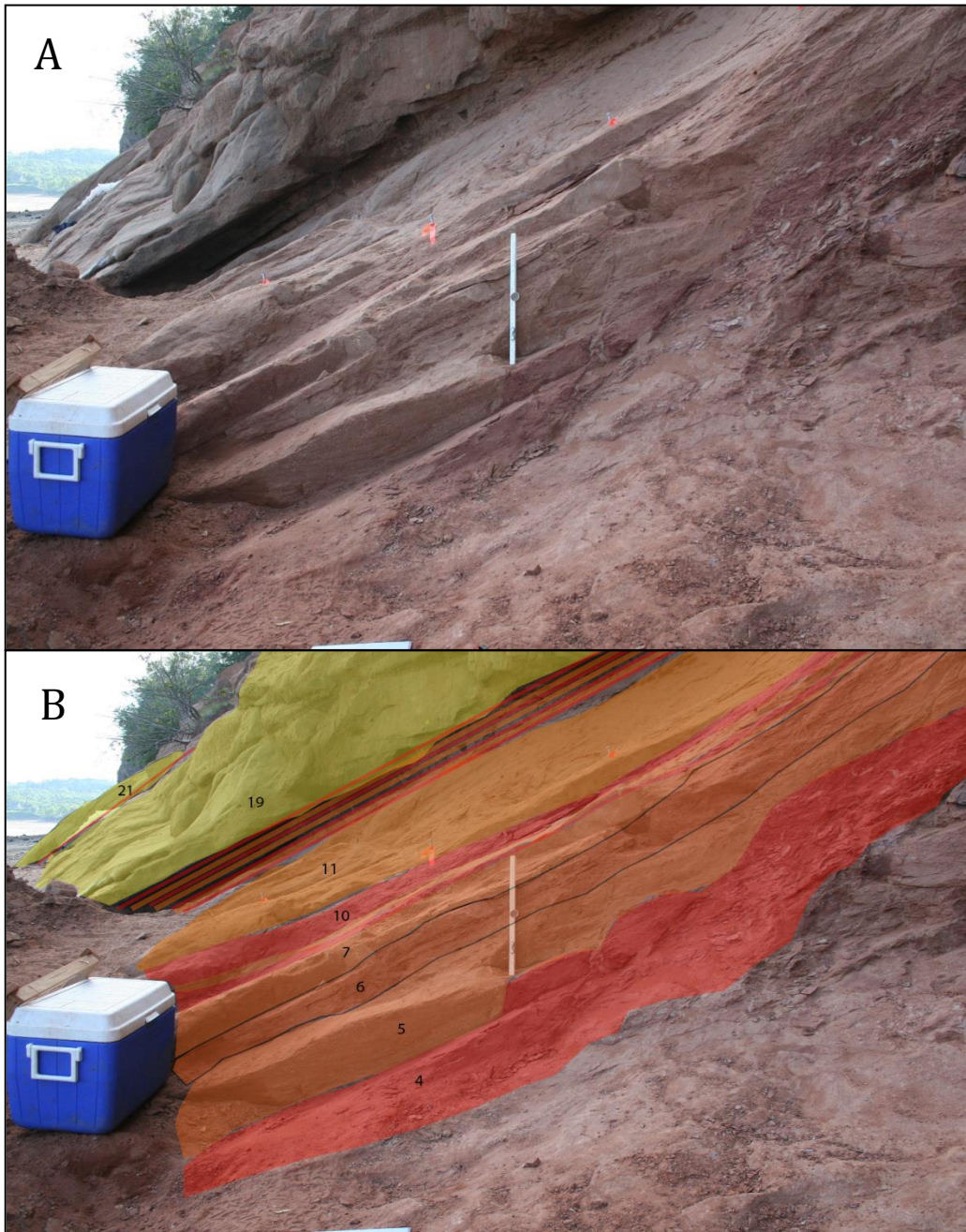


Figure 4.1 The measured section, not annotated (A) and annotated (B). Scale is 50 cm long. Bed numbers shown in B (see Fig. 4.2) Bed colours: Facies 1(mudstone): red; Facies 2 (sandstone): orange; Facies 3 (sandstone): yellow.

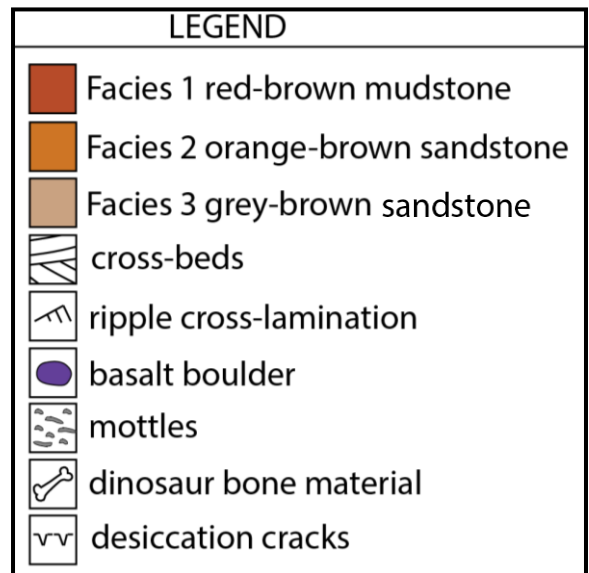
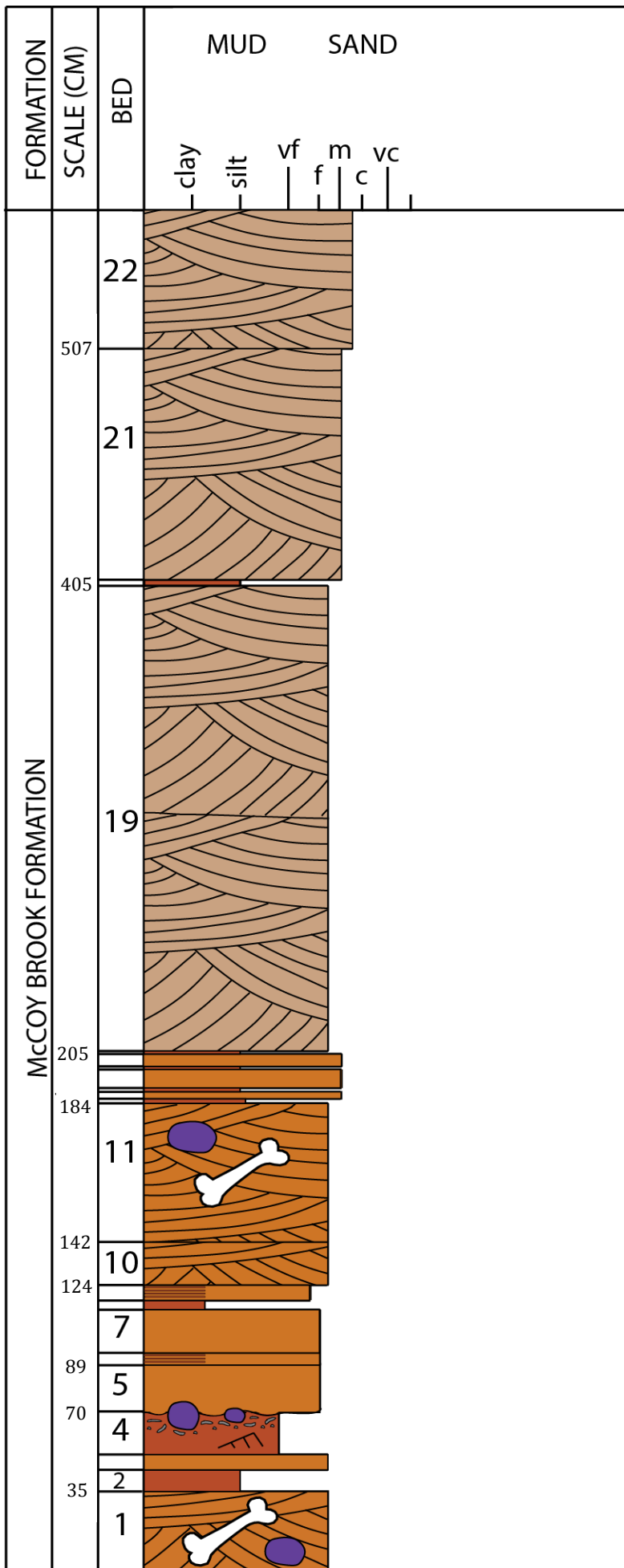


Figure 4.2 Princeton Quarry stratigraphic column.

Facies 1 beds range from 4 to 19 cm in thickness. The majority are fine- to medium-grained silt and incorporate fine- to medium-grained sand. The thickest of these beds, bed 4 (Appendix A) is a 19 cm siltstone that displays unidirectional ripple cross-lamination (Fig. 4.3b), grey-green irregular mottles (Fig. 4.3f), and four sand-filled desiccation cracks on the top surface of the bed (0.5 – 2 cm depth of penetration).

Three mud interbed sections are present in the stratigraphic section, beds 6, 9 and beds 12 through 18 (Fig. 4.2). Beds 6 (Fig. 4.2) and 9 have been labelled as Facies 2 sandstone on the column but contain mud interbeds with 1 cm interbeds of sandstone. Beds 12 through 18 have sandstone beds ranging from 4 to 6 cm thick and have been represented by multiple beds.

The beds do not contain basalt boulders except for the contact between bed 3 and 4, which has a 40 x 25 cm boulder (Fig. 4.3c). This boulder appears to have deformed the top surface of bed 3.

4.3 Facies 2: Orange-brown sandstone

The orange-brown facies has beds that range from fine- to medium grained sandstone. These beds are 4 to 42 cm thick with an average of 29 cm. Most beds display trough cross-bedding, although some beds, especially thinner ones, appear to be massive. Gypsum nodules are common throughout these beds, and have diameters ranging from 1 to 2 mm.

This facies contains prosauropod remains in two beds (beds 1 and 11). The main dinosaur-bearing bone bed, bed 1 (Fig. 4.3e), crops out at beach level and is the lowermost bed within the measured section, with a minimum thickness of 35 cm. The total thickness

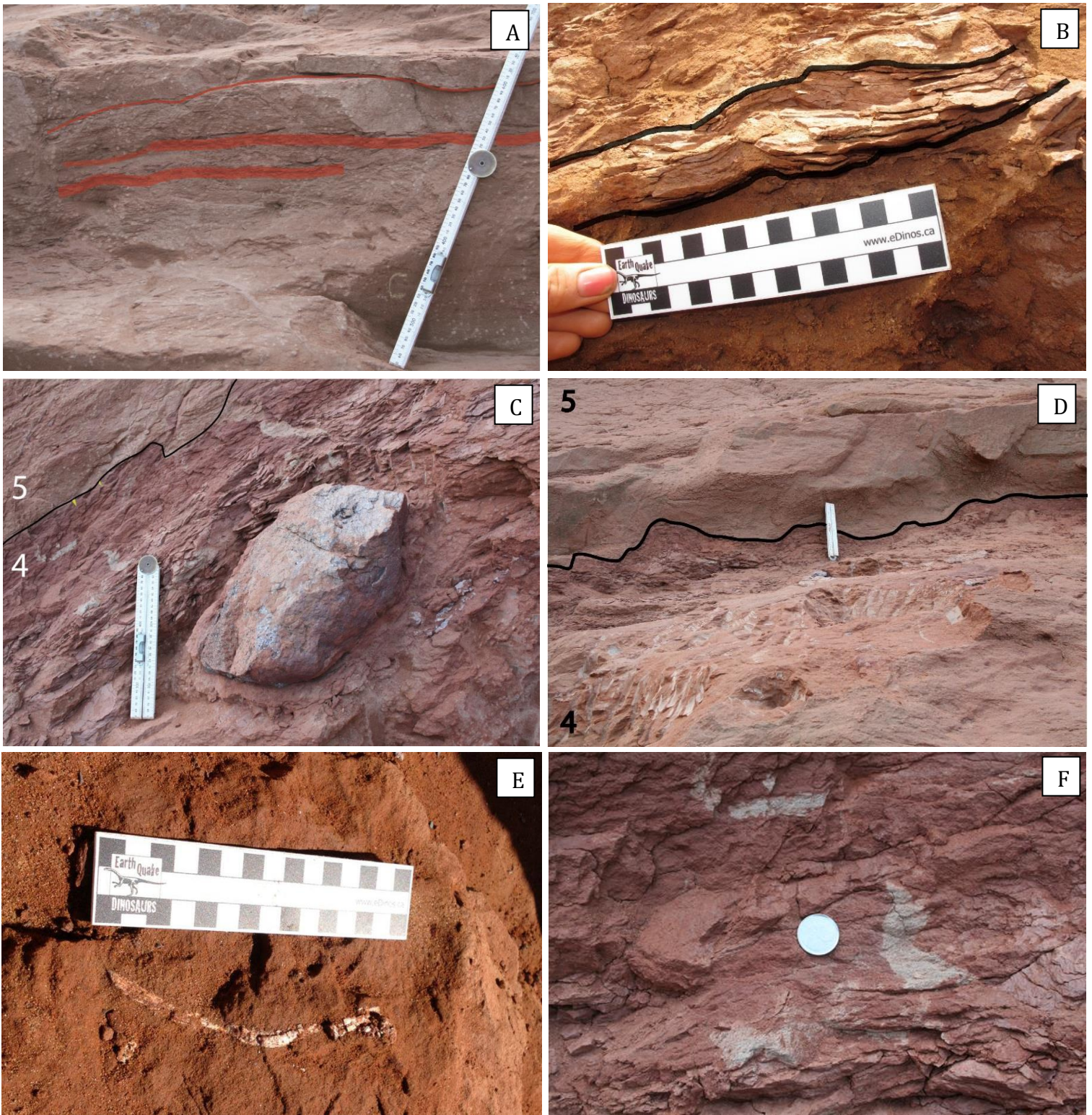


Figure 4.3 Sedimentary features of the measured section, Facies 1 and 2 A) Examples of mud drapes from bed 6, gypsum nodules white spots at lower right B) Ripples cross-lamination from bed 4 C) Basalt boulder and mottling from bed 4. Desiccation cracks indicated by yellow. D) Erosional surface between beds 4 and 5 E) Disarticulated prosauropod rib bone discovered during the 2013 excavation F) Grey-green mottling in bed 4, dime for scale (left side of C).

of the bone-bearing bed is unknown due to faulting, making it difficult to correlate the bed into the cliff face, and beach debris covers a large portion of the bed. During the 2013 excavation, multiple disarticulated bones were found in bed 1 and in a past dig disarticulated bone was found in bed 11. The contact between bed 4 and 5 (Fig. 4.3d) is the only contact in the stratigraphic column that has an erosional rather than linear contact.

4.4 Facies 3: Light grey-brown sandstone

The light grey-brown sandstone facies is a fine- to coarse-grained sandstone with large trough and planar cross-beds (Fig. 4.4), and alternate dark and light lamination (Fig. 4.5). Only three beds in the stratigraphic column are Facies 3 and range from 60 to 200 cm thick, which make up 360 cm of the measured section. Facies 3 contains regularly spaced gypsum nodules throughout, with slightly larger diameters than those in Facies 2, ranging from 2 to 5 mm. The cross-stratified sandstone contains erosional surfaces (Fig. 4.5) where

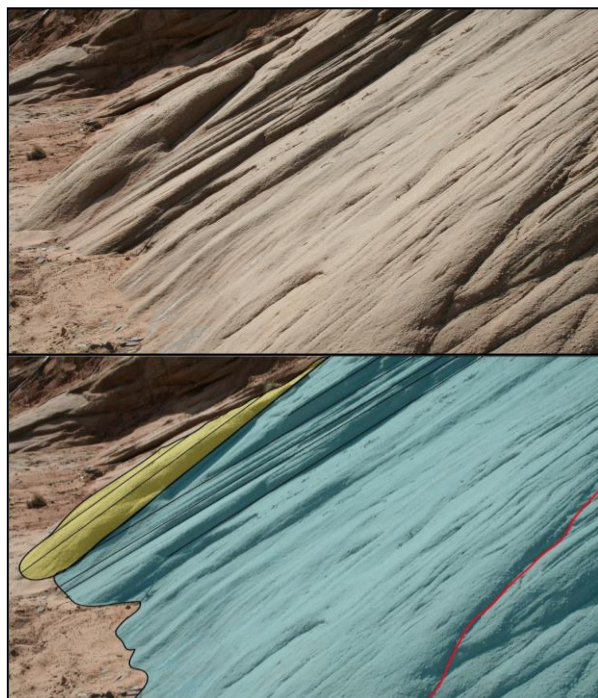


Figure 4.4 Cross-beds from bed 21 (blue) and bed 22 (yellow), Facies 3. Set bounding erosional surfaces defined by red.

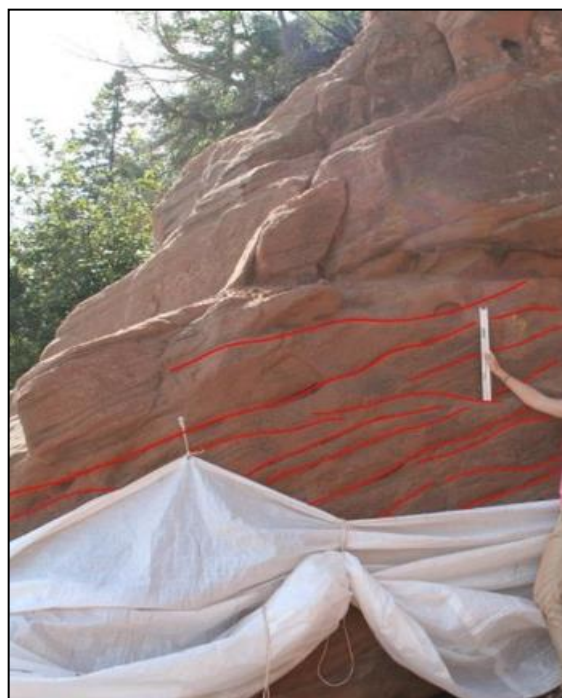


Figure 4.5 Erosional surfaces within bed 21 (Facies 3). Scale is 50 cm long. Note: light and dark lamination on left side.

cross-strata are truncated and overlain by new sets of cross-strata. Cross-sets within the beds range from 20 – 50 cm.

4.5 Facies Associations

On the basis of their distribution in the column, the lithofacies are separated into two facies associations. Orange-brown sandstone (Facies 2) and red-brown mudstone (Facies 1) are interbedded on a centimetre to decimetre scale and termed the Sandstone – Mudstone Facies Association (FA 1). Grey-brown, cross-stratified sandstone (Facies 3) with rare red-brown mudstone (Facies 1) is termed the Cross-stratified Sandstone Facies Association (FA 2). In the measured section, FA 1 is abruptly overlain by FA 2 (Fig. 4.1 and 4.2).

Facies Association 1. This association predominates in the lower part of the section and makes up 205 cm of the stratigraphic column (Fig. 4.2), comprising mainly orange-brown, planar beds of sandstone with layers of thin mud laminae throughout. There are three interbedded sets that have ~3 mudstone laminae per set (Fig. 4.3a). Sandstone comprises 80% of this association with mudstone comprising the remaining 20%. Facies boundaries are abrupt linear contacts with the exception of one contact that has erosional relief (Fig. 4.3d). Basalt boulders are present in this association and are missing in the Cross-stratified Sandstone Association at this site.

Facies Association 2. This facies association predominates in the upper part of the section and makes up 362 cm of strata. The association comprises mainly large-scale trough cross-stratified and planar, grey-brown, sandstone beds of Facies 3 and one 2 cm thick mudstone of Facies 1 with abrupt and linear contacts. Sandstone comprises 99% of this association whereas mudstone comprises only 1%. All beds within this association

appear to be laterally continuous up the cliff face but are deformed intensively by syn-depositional faulting. The mudstone bed that appears within this association is considerably thicker to the east.

To the east of the bone-bed excavation site, on the west side of the ravine that leads from the road to the beach, tabular and planar cross-sets 30-50 cm thick are present. These cross-sets display erosional surfaces and light and dark lamination similar to Facies 3 sandstone. In subsequent chapters, grain size of these cross-bedded sets is compared to grain size within the measured section to determine if they are the same depositional environment. Approximately 10 m east of this ravine, a serrated tooth and sphenodontid mandible (tentatively identified) were found within orange-brown sandstone that contained mud laminae.

4.6 Basalt Boulders

Basalt boulders (Fig. 4.3c) within the strata at Wasson Bluff are remnants of an 8 m high paleo-cliff (Hubert and Mertz, 1984) located to the west of the main bone bed (Fig. 2.3). In the stratigraphic section only three basalt boulders are currently observed, mainly within Facies 2 beds. In the main bone-bearing unit (bed 1), two boulders are present with diameters of 30 and 16 cm. In previous digs basalt boulders have been found in contact with prosauropod fossils (T. Fedak, pers commun., 2014). At the contact between beds 3 and 4 a boulder with 40 cm diameter is present (Fig. 4.3c) and is the only boulder in contact with Facies 1 beds within the stratigraphic column. This boulder appears to have deformed the top surface of bed 3. An approximately 40 cm diameter boulder is present within bed 11, a bed which produced disarticulated bone in the past. Although the measured section depicts accurately the amount of basalt boulders in the studied area, it

does not represent other parts of the cliff face where boulders are more abundant (Fig. 4.5). Basalt boulders in the cliff face also appear to be incorporated into strata similar to Facies 1 mudstone, which does not contain boulders in the stratigraphic section.



Figure 4.5 Cliff face showing basalt boulders in yellow. The red line shows the measured section. Cliff face is 8 m high. The North Mountain Basalt Paleocliff is located to the west of this photo.

Chapter 5: Grain Size Analysis and Petrography

5.1 Grain Size Analysis

5.1.1 Introduction

Of the 22 beds, 16 were sampled and processed. A total of five Facies 1 beds, eight Facies 2 beds and three Facies 3 beds were analyzed. Bed 6, an interbedded sandstone and mudstone unit (Fig. 4.2), was separated into sandstone (6A) and mudstone (6B) samples. A cross-bed set to the east of the excavation site was also sampled and processed to provide a comparison with grain-size of the measured section. Seven beds, 9, 13-18 and 20, were not sampled due to the thinness of the beds: a clean enough sample was not possible to obtain for an accurate grain size analysis because of the very thin interbedded mudstone. When referring to bed numbers, a notation of [Fn] (n=1, 2, 3) is placed after the bed label to describe the facies, for example, bed 21 [F3].

5.1.2 Mean and Distribution

The measured section has grain sizes ranging from 11.3 to -0.38 ϕ , which fall within the ranges of sand, silt and clay. Facies 1 has an average of 56.47% silt, where sand and clay almost equally make up the rest (Fig. 5.1). Mean grain-size ranges from 7.43-5.5 ϕ (silt) (Table 5.1). Facies 2 and 3 are sand dominated with grain size ranges from 3.22-2.53 and 2.11-1.18 ϕ (sand) respectively. Facies 2 has a higher silt and clay fraction than Facies 3 with approximately 11% silt and 5% clay, whereas Facies 3 has approximately 3% silt and 1% clay (Fig. 5.1 and 5.2).

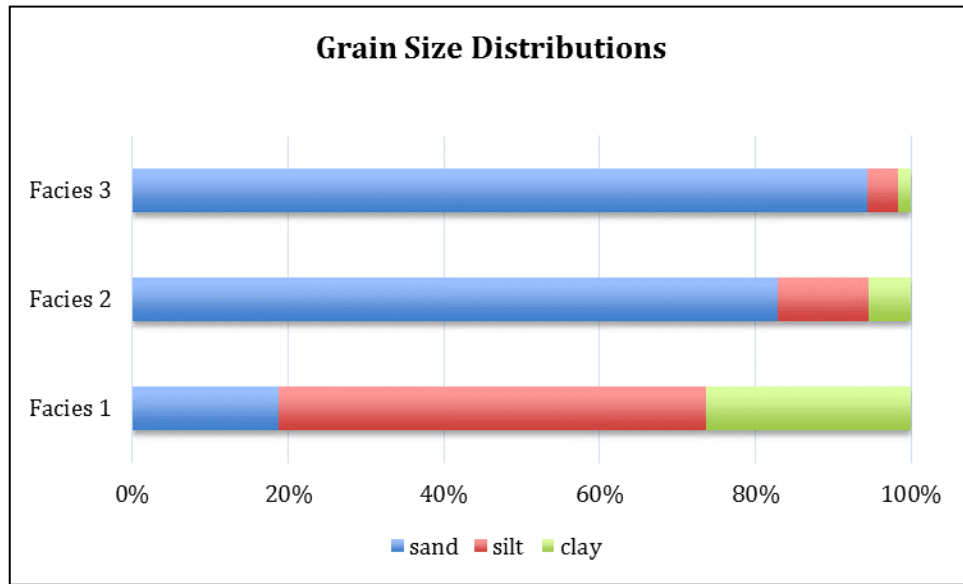


Figure 5.1 Bar graph showing the distribution of sand, silt and clay of the three facies. Data are averages of 5 (Facies 1), 7 (Facies 2) and 3 (Facies 3) samples. Clay and mud were combined from Table 5.1 for this graph.

Table 5.1 Summary of grain size analysis by facies. Terminology based on Folk (1974).

	Facies 1	Facies 2	Facies 3
Number of beds analyzed	5	7	3
Sorting (number of beds)	very poorly (3) poorly (2)	very poorly (3) poorly (4)	poorly (2) moderately well (1)
Mode (number of beds)	unimodal (2) bimodal (2) trimodal (1)	unimodal (7)	unimodal (3)
Grain Size (ϕ)	0.1-11.3	-0.38-11.3	0.12-11.3
Mean (ϕ)	5.50-7.43	2.53-3.22	1.18-2.11
Skewness(ϕ)	-0.22-0.28	0.30-0.63	0.31-0.55
	negative (coarse) to positive (fine)	positive (fine)	positive (fine)
sand (-1 - 4ϕ)	0-38.40%	79.97-85.91%	90.91-97.23%
Silt (4-8ϕ)	40.97-71.97%	10.23-13%	1.19-6.50%
Clay (8-10ϕ)	20.64-33.36%	3.84-6.90%	0.86-2.59%
Mud (4-10ϕ)	61.60-100%	14.09-20.03%	2.77-9.09%

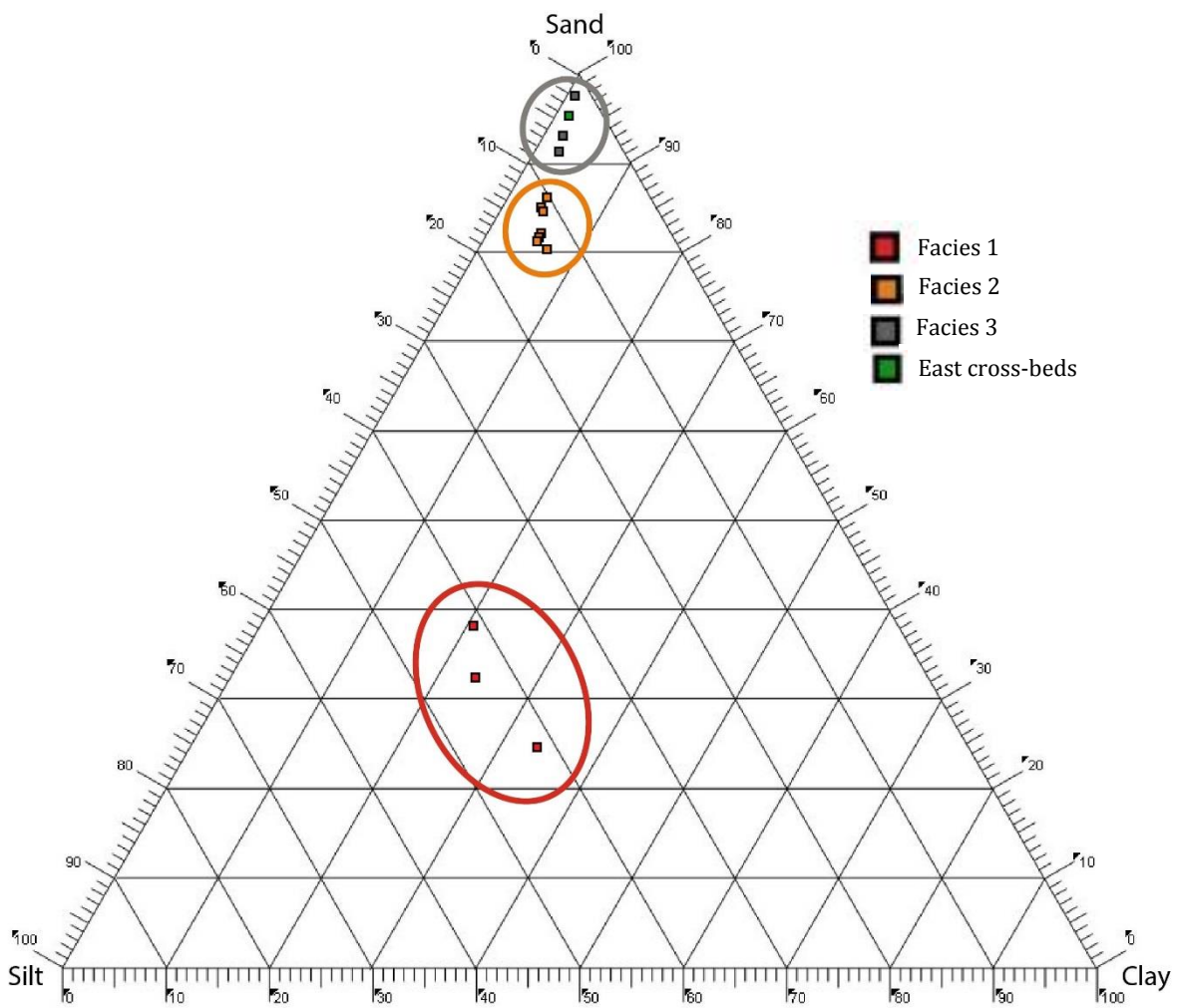


Figure 5.2 Ternary diagram showing distribution of sand, silt and clay in Facies 1, 2, 3 and the east cross-bed set.

5.1.3 Modes

When graphed by particle diameter versus weight percentage, the samples show unimodal, bimodal and trimodal shapes (Fig. 5.3). Facies 1 mudstone displays all three modal shapes with two unimodal samples (Fig. 5.3a, e), two bimodal (Fig. 5.3c, d) and one trimodal sample (Fig. 5.3b). Unimodal beds have a modal apex of 6.5 ϕ , bimodal beds have apices at 7.5-7 ϕ and 2.5-1.5 ϕ and the trimodal sample has apices at 7.5, 5.5 and 2.5 ϕ .

All samples from Facies 2 and 3 are unimodal. Facies 2 samples (Fig. 5.3f-l) have a modal apex ranging from 2-1.5 ϕ , where Facies 3 samples (Fig. 5.3m, n, o), have a modal apex ranging from 1.5-1 ϕ . The east cross-bed set (Fig. 5.3p) is unimodal with an apex at 1 ϕ .

5.1.4 Skewness and Sorting

Terminology is based on Folk (1974). Samples range from negatively to positively skewed. Bimodal, Facies 1 samples (Fig. 5.3c, d) are the only negatively skewed samples in the section. Instead of having a coarse grained tail, these samples have coarse mode. The remaining samples are all positively skewed with a fine grain tail.

Sorting ranges from very poorly to moderately-well sorted with a general trend of better sorting towards the top of the section. Facies 1 is very poorly (bi- and trimodal samples) to poorly sorted (unimodal samples). Facies 2 is also very poorly to poorly sorted. Very poorly sorted Facies 2 samples (Fig. 5.3 f, g) have an obvious fine-grained tail. Facies 3 is poorly to moderately-well sorted. The fine-grained tail in these samples (Fig. 5.3 m n, o) is minimal with the moderately sorted sample (Fig. 5.3o) having the smallest tail and sharpest modal peak. The east cross-beds (Fig. 5.3p) are positively skewed and moderately sorted.

As mentioned in a previous chapter, data from this suite were investigated using Friedman's (1961) plot to distinguish beach, dune and river sands. However, the Wasson Bluff sandstone showed little correspondence with Friedman's plotted areas for river and dune sands. Friedman's study was not able to determine a depositional environment for these samples due to points plotting in the broad dune-river overlap region or not at all within the mean/standard deviation parameters (Fig 5.7). This suite of data is instead compared using Friedman's statement about parameter ranges, rather than his plot, using a combination of mean, sorting and skewness to create scatter plots.

A scatter plot comparing sorting and skewness (Fig. 5.4) shows that all Facies 2 and 3 samples plot at or above 0.3 skewness but are divided at a sorting (standard deviation) of 1.4 with Facies 2 having a higher standard deviation. Facies 1 samples all plot below a skewness of 0.3 and have variable sorting. Mean versus skewness (Fig. 5.5) provides separation at a mean of 2.4, which separates Facies 2 and 3, with Facies 2 displaying higher mean phi values (smaller grain-size). Facies 3 plots above a mean of 5.2 (larger grain-size). A comparison of mean and sorting (Fig 5.6) provides an excellent separation of facies, showing the sorting and mean values which divide Facies 2 and 3 as previously mentioned. This graph clearly displays that Facies 3 has a larger phi values (smaller mean) and is better sorted (smaller standard deviation) than Facies 2. In each graph the east cross-beds plot among Facies 3 samples. Friedman's plots show trends of river sands having a higher standard deviation and mean relative to dune sands. The suite of data for this study displays a similar trend, interpreted in a later section to indicate fluvial and eolian sediments.

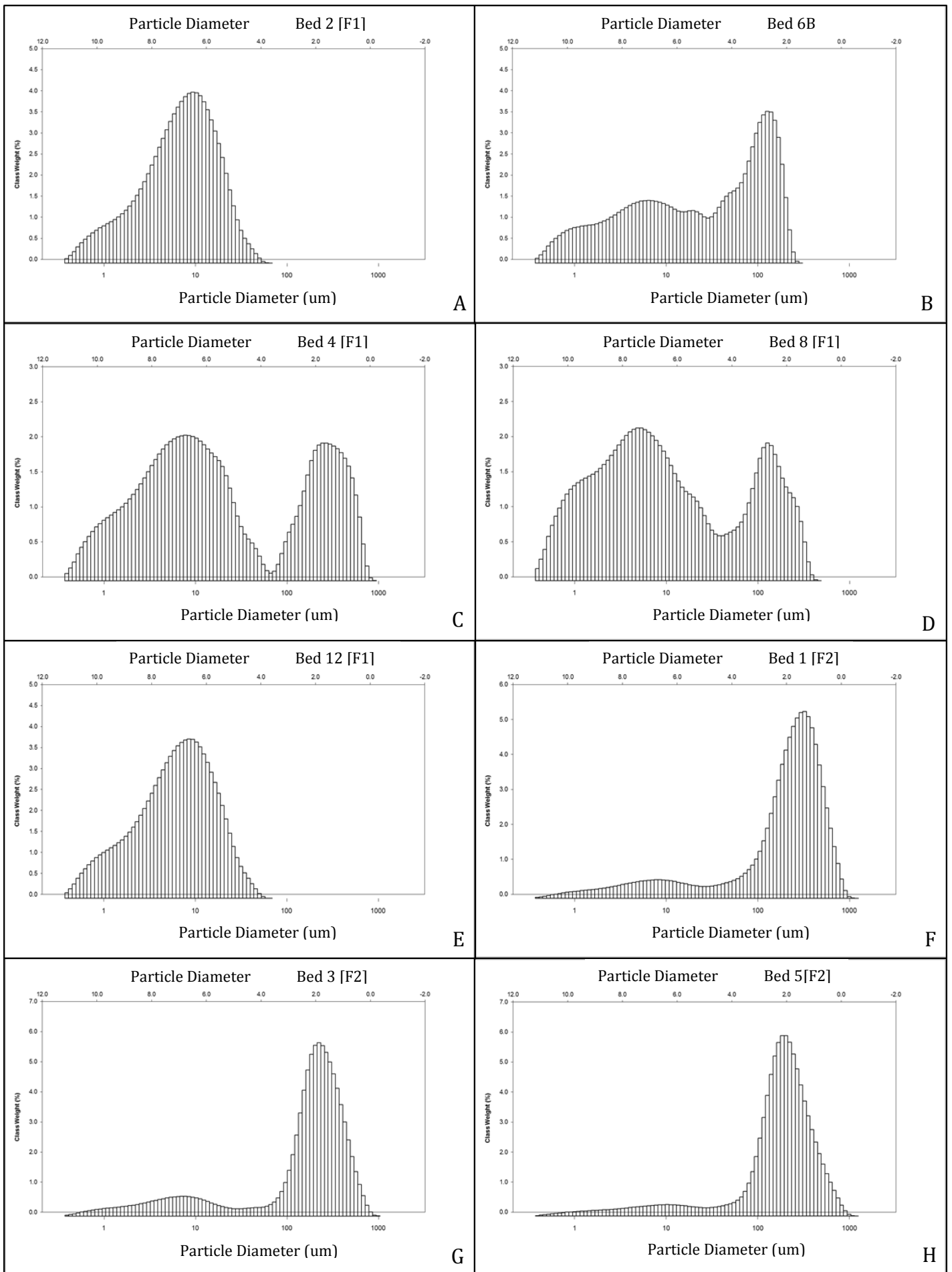


Figure 5.3 Histograms showing grain-size distribution. Histograms are grouped by facies.

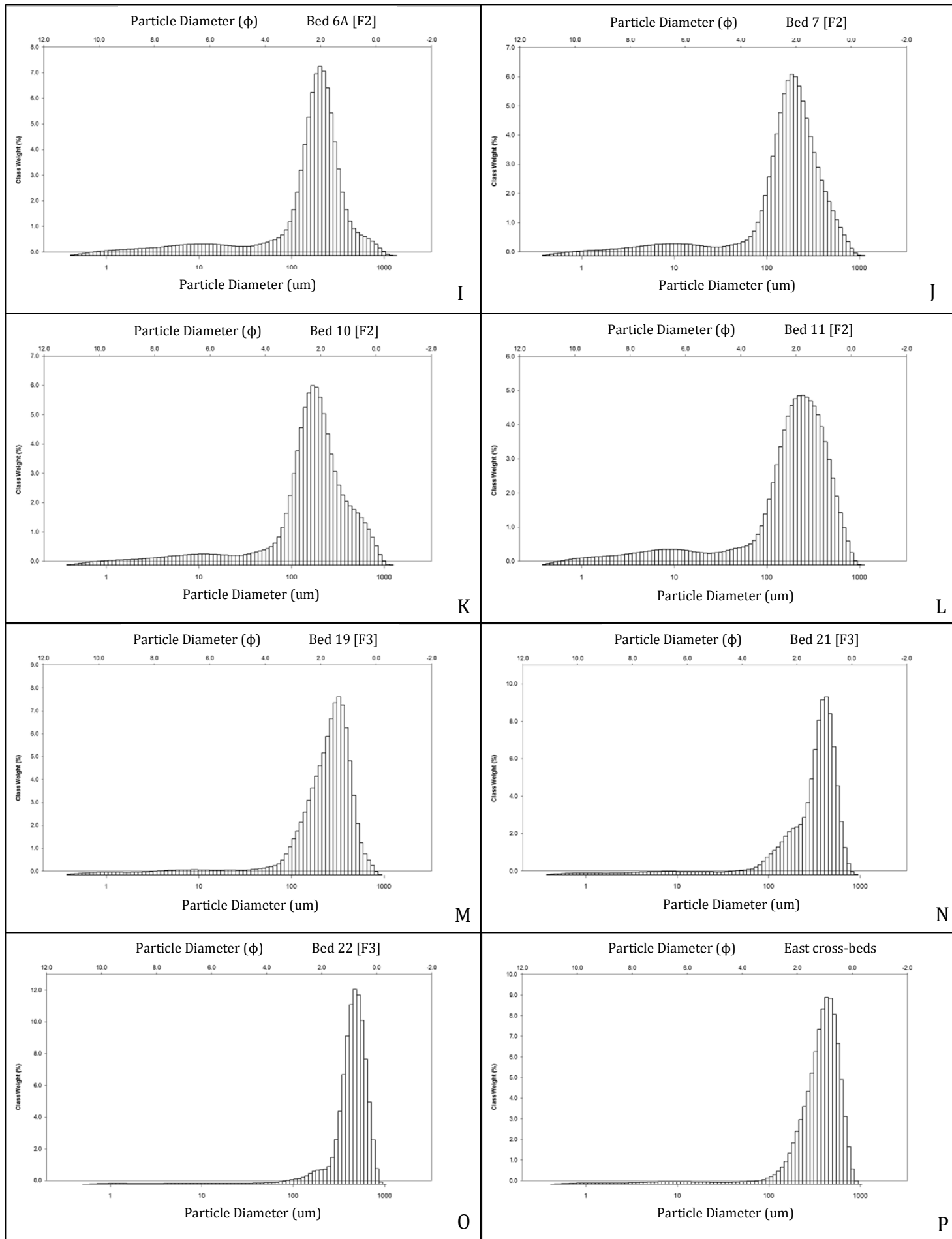


Figure 5.3 Continuation of histograms showing grain size distribution. Histograms are grouped by facies.

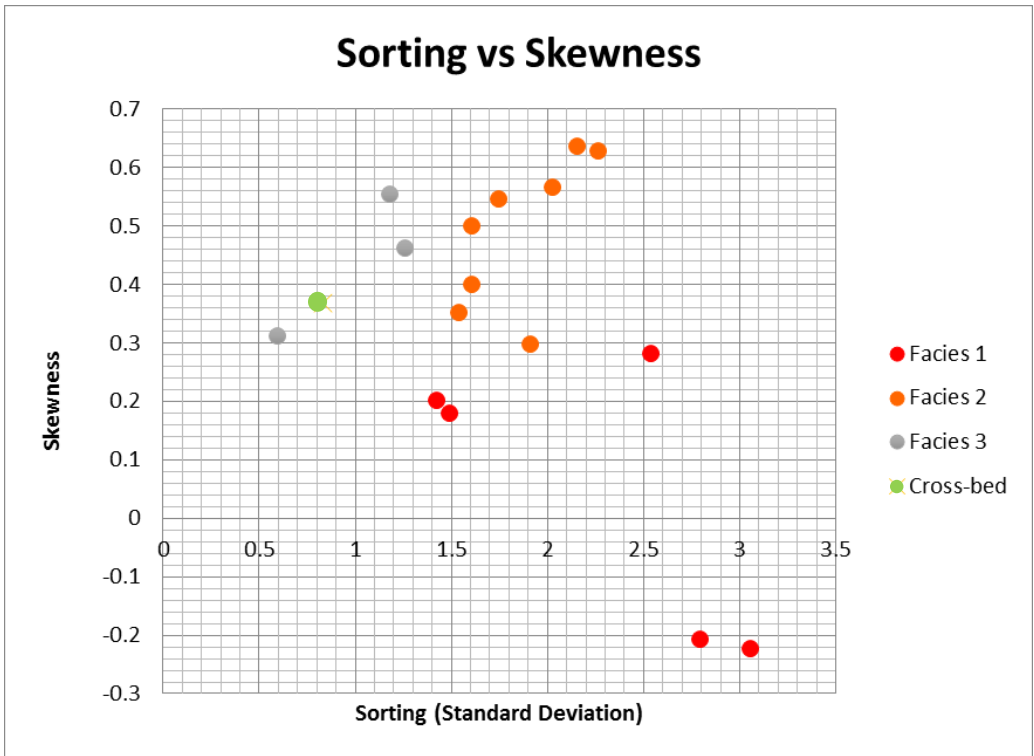


Figure 5.4 Scatter plot showing the relationship between sorting and skewness. Units in phi.

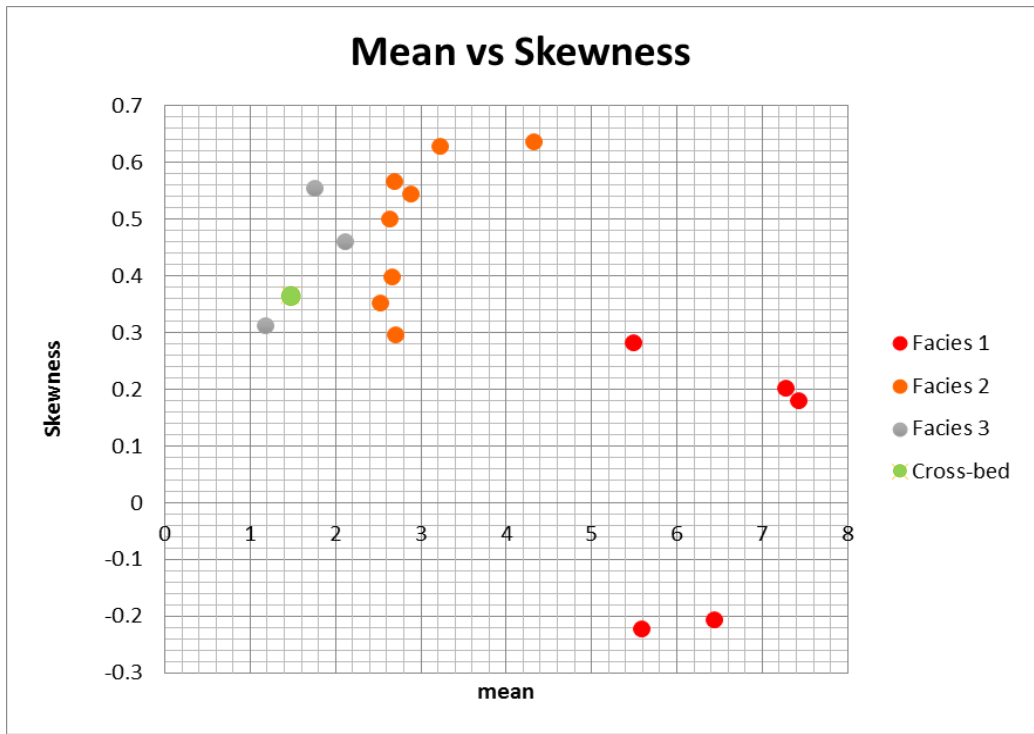


Figure 5.5 Scatter plot showing the relationship between grain size and skewness. Units are in phi.

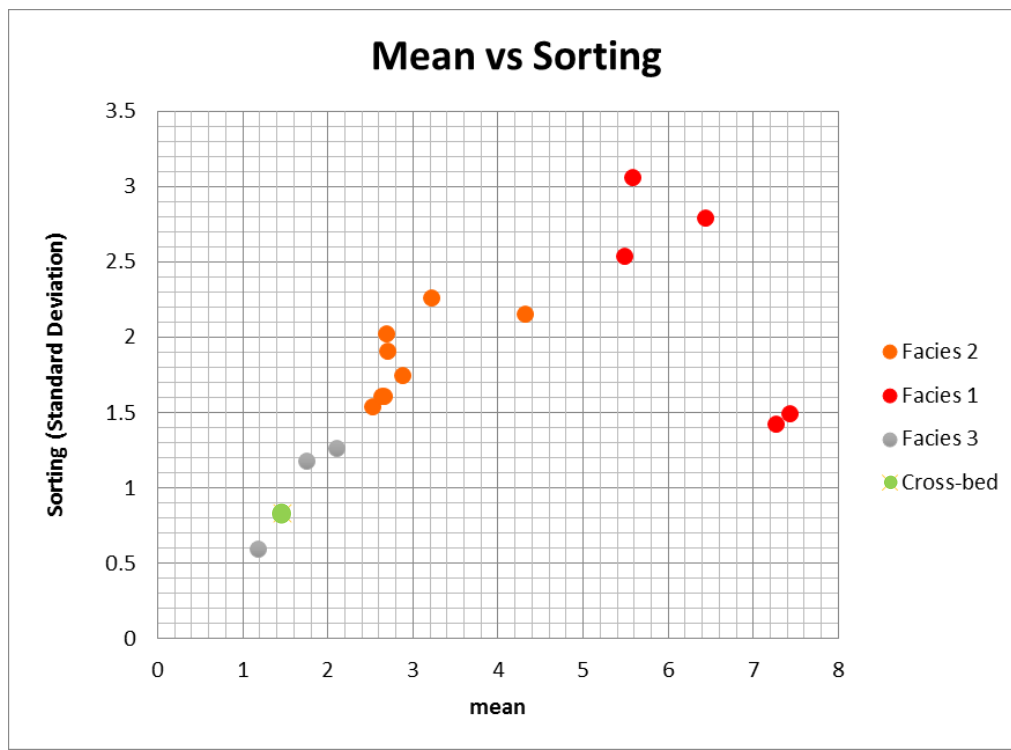


Figure 5.6 Scatter plot showing the relationship between mean and sorting. Units in phi.

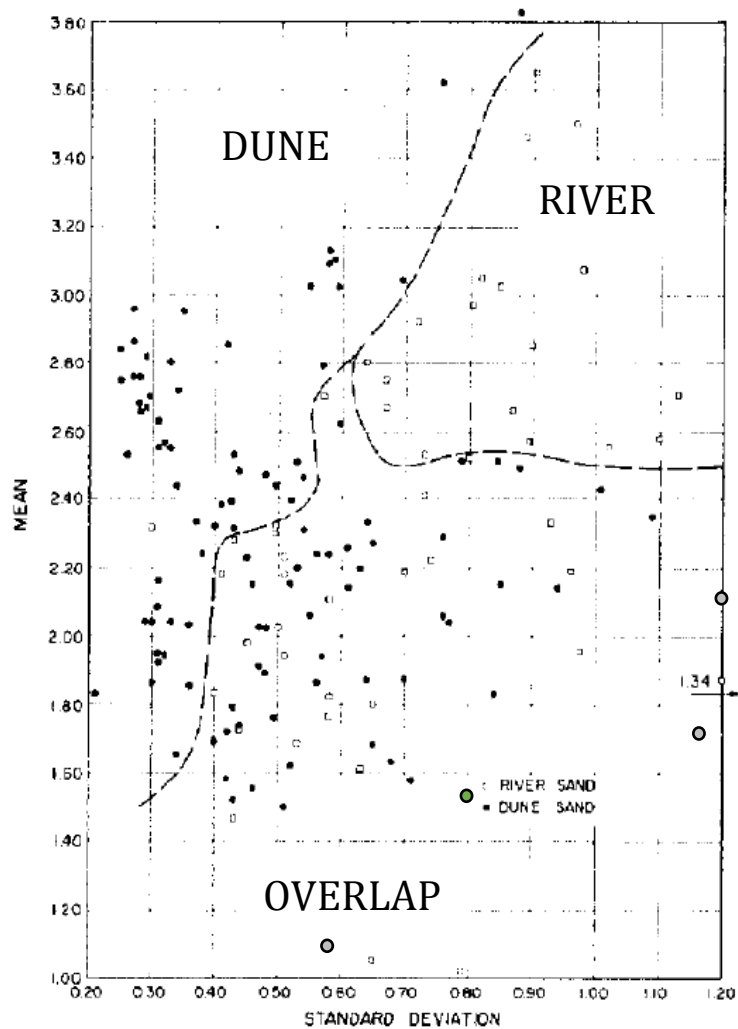


Figure 5.7 Facies 3 (grey) and the east cross-bed set (green) is plotted using Friedman's (1961) boundaries of modern river and dune sand. Facies 1 and 2 did not plot within the parameters of this graph. See figure 5.6 for full plot.

5.2 Petrographic Analysis

Point counting did not yield a distinct separation of facies based on composition. From the seven samples analyzed, six were Facies 2 and one was Facies 3. The samples plot within the feldspathic litharenite and lithic arkose fields on a quartz-feldspar-lithic ternary diagram (Fig 5.8).

One of the field criteria to distinguish facies was colour. In thin section, Facies 2 had more clay matrix and iron oxide coating the grains, likely hematite, compared to Facies 3. This is consistent with the orange-brown colour assigned to Facies 2 and grey-brown colour assigned to Facies 3 in the field. Clay present is chlorite and likely also includes illite and possibly smectite (due to the cracking of collected bones after they dry), but identification of clays is difficult due to the fine-grained nature of the sediment. Grain size analysis determined that Facies 3 has better sorting and coarser grains than Facies 2. A petrologic comparison of the two facies by grain size (Fig. 5.9a, b) corresponds with the grain-size data. Facies 3 laminae, observed in the field, are distinguished by partitioning of oxide grains from quartz and feldspars grains and are also observed in thin section (Fig. 5.9b).

Grain-size analysis yielded two bimodal grain-size distribution plots from Facies 1 samples (Fig 5.3c, d). In thin section, the sand component is observed concentrated and scattered in a reddish clay (Fig. 5.9c). Very poorly- to poorly sorted Facies 2 samples, as determined by grain-size analysis are consistent with out-sized grains of well-rounded quartz and feldspar in bed 7 (Fig. 5.9d), suggesting that part of the poorer sorting represents an added population of unusually large grains.

Detrital and lithic grains include: rock fragments of sandstone, mudstone, chert and schist (Fig. 5.10e, f) as well as quartz, plagioclase, microcline (Fig. 5.10a), muscovite, olivine (Fig. 5.10b), orthopyroxene (Fig. 5.10c), garnet (Fig. 5.10d), and tourmaline detrital grains (Table 5.2). Sandstone, mudstone and chert were the predominated rock fragments, few schist fragments were observed. Only one grain of orthopyroxene was observed and no gypsum nodules were observed in thin section.

Grain contacts are floating and concavo-convex with muscovite (Fig. 5.9e) kinked between grains. Polycrystalline quartz has sutured quartz crystals that make up the detrital grain (Fig. 5.9f). The margins of some quartz, feldspar and lithic grains are corroded. Plagioclase and microcline grains have undergone sericite alteration (Fig. 5.10a), in some cases making identification difficult.

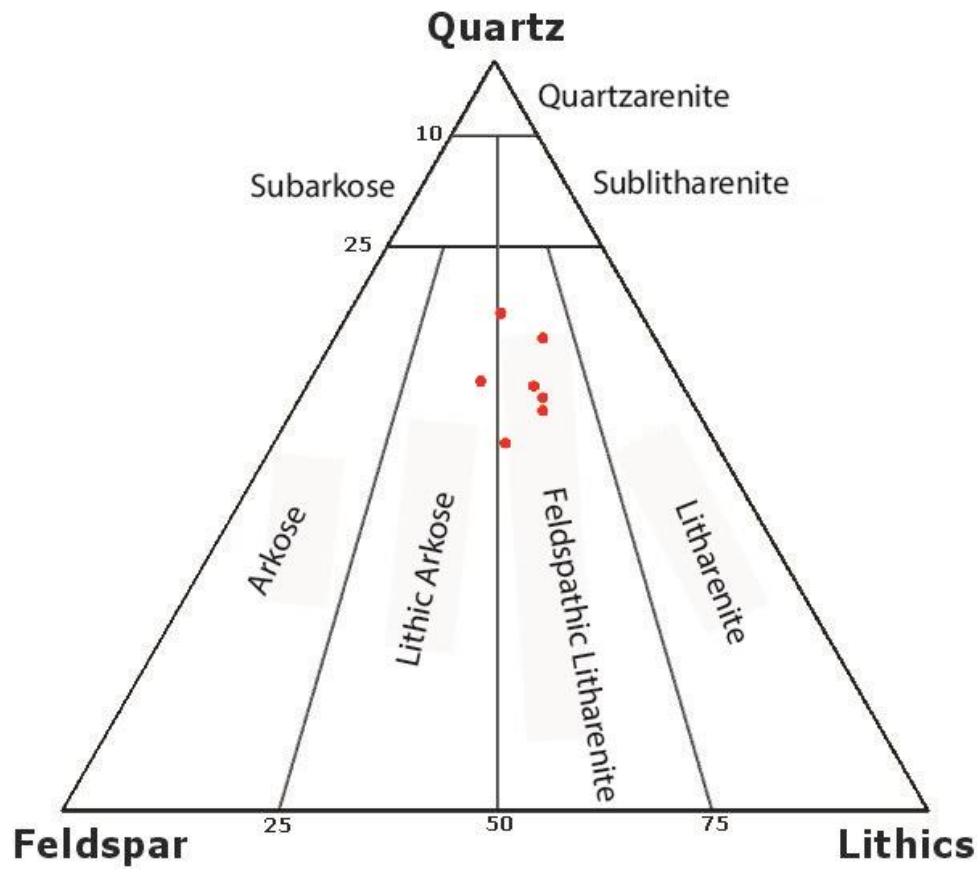


Figure 5.8 Composition of seven samples based on point counting analysis. The sample plotting in the lithic arkose field is Facies 2. Sandstone classification of Folk (1974).

Table 5.2 Summary of detrital minerals and lithic grains in Facies 2 and 3

	Facies 2	Facies 3
Minerals	Quartz - monocrystalline	
	Quartz - polycrystalline	
	Plagioclase	
	Microcline	
	Garnet	
	Clays	
	Muscovite	
	Biotite	
	Chlorite	
	Hematite	
	Tourmaline	
	Rutile	
	Oxide	
	Zircon	
Lithics	Olivine	Orthopyroxene
	Sandstone	
	Mudstone	
	Schist	
	Chert	

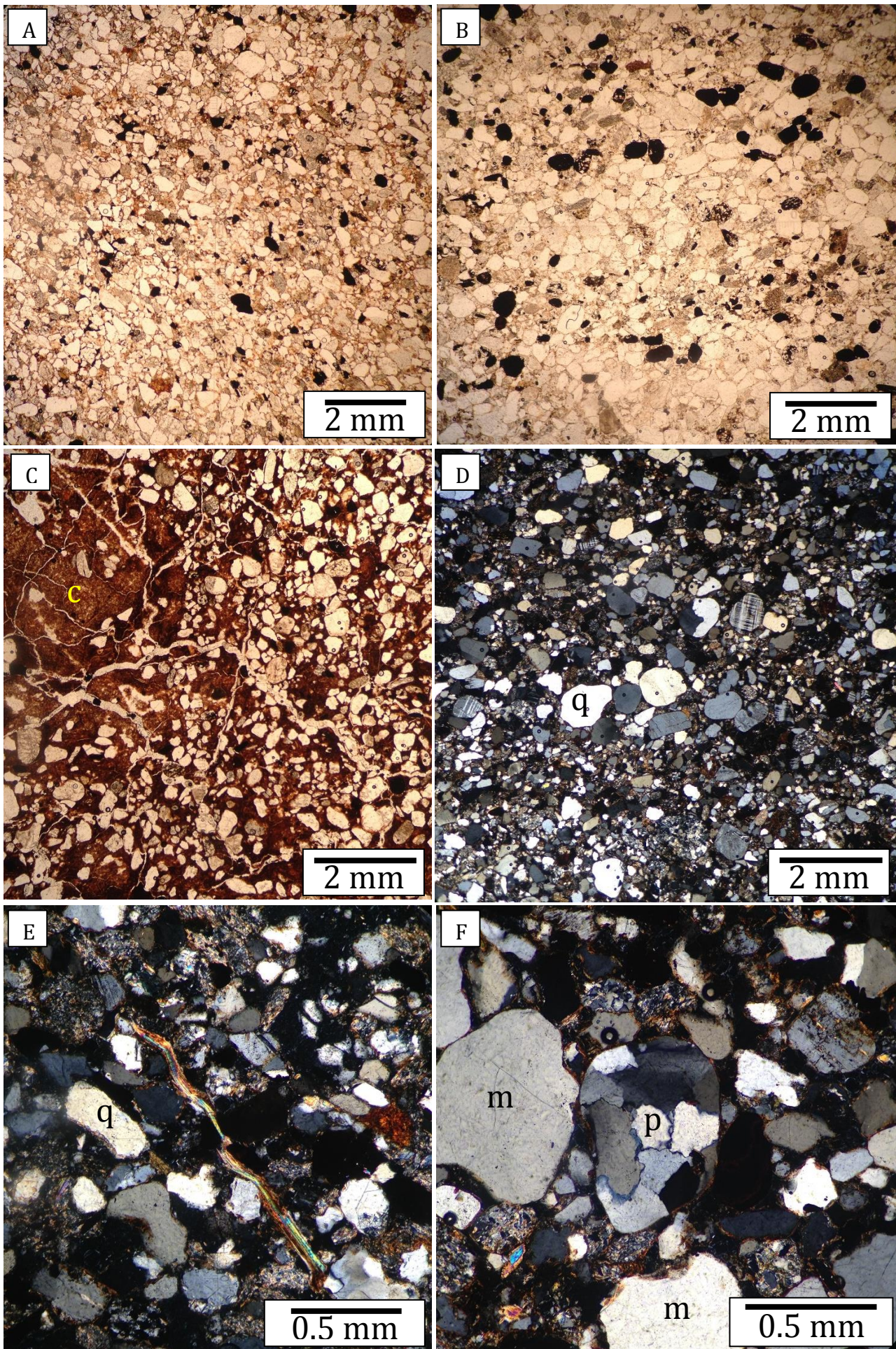


Figure 5.9 Examples of facies and detrital grains. A) Bed 3 [F2] B) Bed 21 [F3], coarse grains and better sorted than bed 3. Dark minerals are opaques. C) Bed 4 [F1] shows silt- and sand-sized grains concentrated in reddish clay (c). Anastomosing cracks are artifacts of section manufacture. D) Well-rounded, outsized quartz (q) and microcline grain in bed 7 [F2]. E) Deformed mica grain from bed 10, Facies 2. F) Mono- (m) and polycrystalline (p) quartz grain from bed 7 [F2].

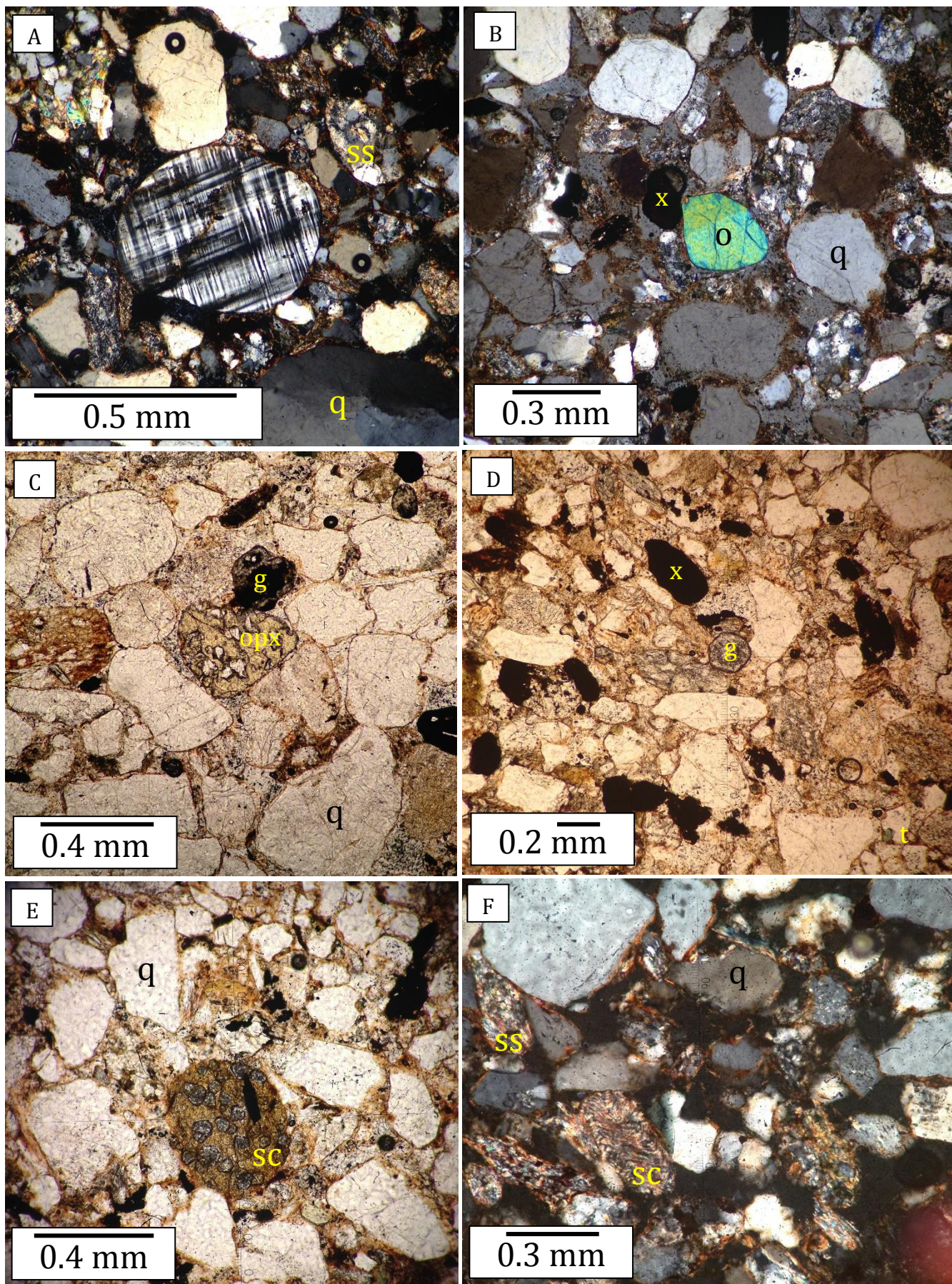


Figure 5.10 Examples of detrital and lithic grains. A) Microcline grain from bed 7 [F2] with seritization. B) Olivine (o) grain from bed 1 [F2]. C) Orthopyroxene (opx) from bed 21 [F3]. D) Sub-euhedral garnet (g) from bed 10 [F2]. E) Schist lithic (sc) grain with garnet overprinting faint foliation from bed 10 [F2]. F) Schist lithic with preserved foliation defined by mica from bed 10 [F2]. A, B and F under cross-polarized light. C, D and E under plane-polarized light. q: quartz, ss: sandstone, t: tourmaline, x: oxide.

Chapter 6: Discussion

6.1 Interpretations

6.1.1 Facies Association 1

Facies Association 1 predominates in the lower part of the stratigraphic section and is characterized by ripple cross-lamination, mud laminae, small scale trough-cross beds, planar stratification, and an erosional surface. This facies association suggests a fluvial succession that experienced episodic lower flow regime drainage, creating packages of sand with intervening mud drapes. No channel scours were observed within the measured section making channel dimensions difficult to estimate.

Within Facies Association 1, three packages of Facies 1 mudstone laminae are interbedded with thin beds of Facies 2 sandstone. Each package contains 3 to 4 mudstone laminae with abrupt contacts. This interbedded nature suggests repeated waning flow from moderate to low velocities, allowing deposition of thin sand beds followed by settling of mud (Fig. 4.3a).

Bed 4 [F1] is a 19 cm mud unit that displays many of the features that characterize Facies Association 1 and is the only bed in the section where ripple cross-lamination, grey-green mottling, an erosional surface and desiccation cracks are present. Ripple cross-lamination suggest that flow was north-east to south-west. The bimodality of bed 4 (Fig. 5.3c) indicates that there is a sand component within this mudstone bed, which is also supported by petrography. The apex of the sand component is 1.5 ϕ , similar to the apices of Facies 2. This implies there was interaction between the two facies. The surface of bed 4 is erosional (Fig. 4.3d) suggesting there was a stronger flow that deposited bed 5, eroding the surface of bed 4. Desiccation cracks on the surface of bed 4 suggest that there was sufficient

time between the deposition of beds 4 and 5 to allow the surface of bed 4 to dry out and crack. Bed 5 [F2] then infilled these cracks and represents the next episode of flow. Only four desiccation cracks were visible on this surface and they are fairly small (0.5 – 2 cm depth of penetration); other desiccation cracks were probably eroded away. Outsized rounded grains of plagioclase and quartz suggest eolian additions to the fluvial sediment.

6.1.2 Facies Association 2

Facies Association 2 is characterized by large-scale trough cross-bedding with one 2-cm mud bed that is weakly stratified. The sediment is moderately sorted and is better sorted up section with the best sorted sediment in the topmost bed 22. These sedimentary structures and better sorting compared to Facies Association 1 imply a deposition by eolian processes. Distribution curves of Facies 3 also support an eolian deposition, as the skewness and shape of the curves are often attributed to eolian deposition (Folk, 1971). The thin mud bed within this association may represent a flood deposit.

Due to the similarity of grain-size distribution and sedimentary structures (cross-beds and light/dark laminae) of the cross-beds on the east side of the main bone bed, they can be considered equivalent to Facies Association 2 and interpreted as an eolian depositional environment. They may also be laterally equivalent to beds 19, 21 or 22, although this is difficult to assess due to faulting. With other outcrops of eolian strata further to the east, it becomes apparent that the fluvial Facies Association 1 has been deposited between eolian dune successions. Dark and light laminations noted in the Wolfville Formation by Hubert and Mertz (1984) are attributed to grainflow (quartz-rich) and grainfall (fine grained, oxide-rich). Laminations in the eolian dunes at Wasson Bluff are determined to form by these same processes.

6.1.3 Early Burial History

The sandstones of Facies Associations 1 and 2 have been minimally compacted indicated by floating and concavo-convex contacts and kinking of mica grains. Sandstones, which are easily disaggregated have a clay matrix and are poorly to moderately cemented by gypsum to form small nodules. No quartz overgrowths were identified, indicating a lack of silica cementation during diagenesis. Among other sources, a source of silica for silica cementation can come from silica dust which might be expected with eolian deposition but because most grains are not well rounded and sandstones are immature: there may not have been enough abrasion to create silica dust (8-14 ϕ). Clays present are conceivably illite and smectite which would form variously from the decomposition of mica, feldspar and lithic components. The presence of smectite is inferred due to some bone specimens cracking after they are extracted from the sediment and have dried (T. Fedak, pers commun., 2013). Corrosion of grains occurred during early diagenesis and grains were then coated with hematite and clays. Although there was minimal compaction some bones were affected by crushing due to minimal permineralization of the bones and deformed by syn-sedimentary faults (Fedak, 2006).

6.1.4 Grain Size Analysis

Grain-size analysis shows that the three facies have distinctive properties, with Facies 3 sands coarser and better sorted than Facies 2 sands. The method supports a division between water-laid (FA 1) and wind-laid (FA 2) sands in the measured section. Grain-size data plots based on the boundaries proposed by Friedman (1961) separating dune, beach and river sands did not provide insight into the depositional environment at Wasson Bluff. However, comparison of the grain-size distribution between Facies 1, 2 and 3

provided a quantitative separation between the facies. It may be possible to provide identification of facies for a sample from other areas of Wasson Bluff using grain size analysis although field and petrologic observations in conjunction with grain size analysis would yield the best results.

6.1.5 Gypsum Nodules, Iron Oxidation and Mottling

Authigenic gypsum nodules are present through the section in Facies 2 and 3 and envelop other grains rather than forming detrital clasts. The nodules range in size from 1 to 5 mm and are regularly spaced at 0.5 to 2 cm. The nodules likely represent diagenetic interaction of groundwater with already deposited fluvial and eolian sandstone. Although the timing of nodule formation could not be constrained in the present study, the presence of gypsum nodules throughout the section is in accord with a relatively arid climate, as indicated by eolian deposition and supported by the arid climate assessment of Frakes (1979).

Facies Association 1 comprises red-brown mudstone and orange-brown sandstone. This colour range is probably the product of iron-oxidization and precipitation of hematite on grain surfaces. Formation of hematite grain coatings likely occurred during early diagenesis. This colour is not surprising as it is characteristic of many sandstone beds that were deposited in an arid to semi-arid climate (Morton and Hallsworth, 1999). Iron that became oxidized may have come from a variety of ways including being brought in by freshwater, weathering, soil development or biological effects. Dissolution of certain minerals may also contribute iron and will be discussed in a subsequent section. Hematite and clay coated grains also support ground water interaction.

The mottles present in bed 4 are common in near-surface sediments and are linked to variable groundwater levels. During high groundwater levels, oxygen is not able to penetrate the sediment and reduced mottles are the result. Mottles support groundwater interaction with the sediments as suggested earlier by the presence of gypsum nodules.

6.1.6 Provenance

There is no obvious separation of facies based on the composition of the sandstones, implying that they are genetically related and sourced from the same area. Due to the slightly better sorting of Facies 3 as compared to Facies 2, it is reasonable to infer that the sediment composing these sandstones was brought into the basin by some process and then redistributed to their respective beds. Fluvial processes probably carried the sand into the basin during wetter periods, and the sand would then have been redistributed by eolian processes, resulting in a slight change in grain-size parameters but relatively little change in overall composition.

Sub-angular grains and the presence of lithic grains (Fig. 5.10), microcline, plagioclase, and orthopyroxene also indicate a proximal source and immature sandstone. Orthopyroxene does not easily withstand erosion and weathering events and is quickly eliminated from sandstones as they are reworked and become mature. In red-bed forming environments, dissolution of orthopyroxene, clinopyroxene and calcic amphiboles is extensive allowing the iron in solution to become oxidized, creating another source for the classic red-bed (Morton and Hallsworth, 1999). Orthopyroxene (Fig. 5.10c) was identified in bed 21, a Facies 3, eolian bed. The grey-brown colour of this bed may imply that dissolution was not as strong a factor in eolian beds relative to fluvial beds as eolian beds have less interaction with water, allowing orthopyroxene to survive longer than it would

have in fluvial beds. However, only one orthopyroxene grain has been identified in thin section.

Detrital schist fragments with and without euhedral garnets (Fig. 5.10e and f) are present, some of which still have their foliation preserved. These grains are attributed to a metamorphic source within the Cobequid Highlands. Polycrystalline quartz, composed of several quartz crystals that have sutured grain contacts also imply a metamorphic origin. Additions of igneous detrital minerals is also likely due to the presence of oxides, olivine, tourmaline, altered plagioclase and microcline and the close proximity of the North Mountain Basalt. The timing of sericite alternation from plagioclase and microcline is difficult to constrain but could have happened before diagenesis. These grains probably would have been able to survive transport and be incorporated into sandstone because of the proximal source.

The Minas subbasin was formed through transtension from the reactivation of the sinistral Cobequid Fault. The fault (and beginning of the Cobequid Highlands) is located approximately 10 km north of Wasson Bluff making the Cobequid Highlands a proximal source for the McCoy Brook Formation.

6.1.7 Basalt Boulders

In the measured section boulders appear to be correlated with bone as boulders are prominent in the Facies 2 bone-bearing sandstone beds. This correlation is probably just timely emplacement of boulders as a stochastic process. Elsewhere in the cliff face they also appear to be present in Facies 1 and 3 (although, not seen in the stratigraphic section), along with Facies 2. Hubert and Mertz (1984) suggested that basalt boulders veneer first-order surfaces of eolian dunes and, although this may be true elsewhere, it does not appear

to be the case within the measured section. Basalt boulders appear to have been eroded from the paleocliff sporadically and emplaced within the adjacent sediment. In the measured section, boulders are only seen with Facies Association 2, which could be due to higher erosion or transport rates as this drainage system flowed through the dune field. Tanner and Hubert (1991) discuss basalt breccias and conglomerates representing talus and debris flow deposits in the McCoy Brook Formation. Both of these deposits are clast supported with abundant basalt boulders originating from basaltic cliffs. Basalt boulders at the Princeton Quarry are isolated boulders within fluvial and eolian sediment (as represented by the cliff face) and do not represent talus or debris flow deposits but do originate from the same source.

6.1.8 Paleoenvironment

Based on an interpretation of the facies associations at Wasson Bluff, the prosauropod bones were preserved within a fluvial drainage system (FA 1) that flowed through an active dune field (FA 2) (Fig. 6.1, 6.2). Trough cross-bedding in fluvial Facies 2 suggests an actively flowing system during wet periods rather than passive flooding of an interdune area. This drainage system experienced episodic flow and waning velocities, as indicated by the interbedding of mudstone and sandstone within Facies Association 1. The largest cross-set in Facies Association 2 was 30 cm high, giving the eolian dunes a minimum height. Hubert and Mertz suggest (1991) 3 m, although truncated tops of the preserved cross-beds make it difficult to infer original dune height and may have been 3 to 10 m high. The paleo-wind direction was 241° which formed barchans and barchanoid ridges (Hubert and Mertz, 1991). Due to the small measured section at the Princeton Quarry site, a reliable paleo-wind direction and dune geometry was unattainable.

Due to the lack of evidence for root traces these dunes were probably not stabilized by vegetation. In a dune field with small dunes and little vegetation, it is likely that fluvial successions would have traversed the area as braided rivers or sheet flows, as observed in many modern dune fields (Langford, 1989). Within the measured section, only a small area of fluvial-eolian interaction is visible. The fluvial succession was covered by advancing dunes that may have laterally displaced the drainage system.

Approximately 20 m east of the Princeton Quarry bone bed, a serrated tooth and sphenodontid (tentatively identified) skeletal remains were found within orange-brown sandstone interbedded with mud laminae during the 2013 excavation. These beds may be considered similar in depositional environment to Facies 1 and 2 (FA 1) and could represent another local fluvial system within the dune field (Fig. 6.2). This area is also associated with a thick mud bed (~20 cm). At the eastern margin of the half-graben, lacustrine (fish bed) strata followed by fluvial successions were laid down on top of the undulating surface of the North Mountain Basalt (Price, 2014). These strata represent a transition from a lake environment to fluvial deposition and were finally covered by eolian strata that underlie the excavation site (Fig. 6.1).

On a large scale, subsidence associated with this half-graben allowed sediment to accumulate on the top surface of the North Mountain Basalt, with a large volume of eolian sediment that was probably brought down from the Cobequid Highlands initially in rivers.

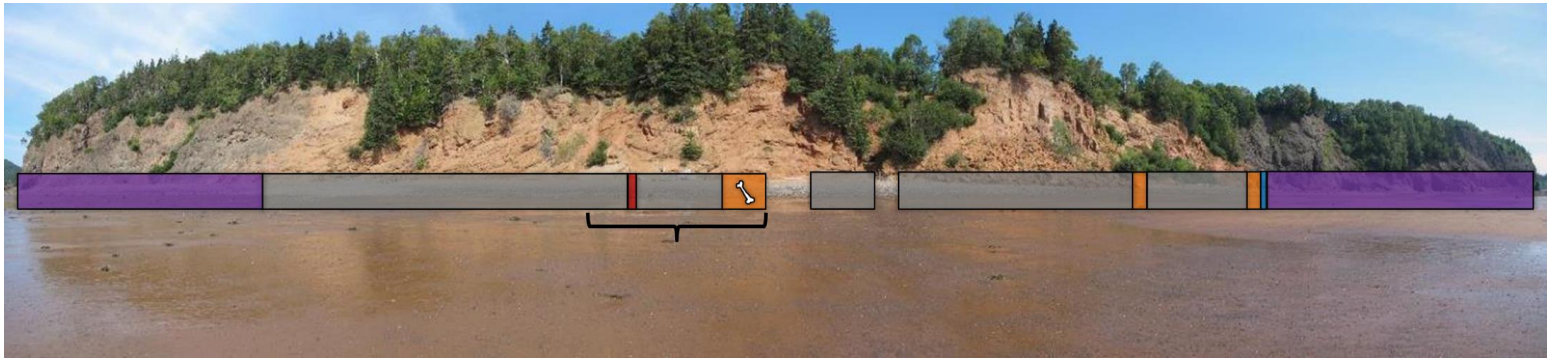


Figure 6.1 Wasson Bluff annotated with facies interpretation. Purple = North Mountain Basalt, blue = lacustrine, orange = fluvial sandstone, grey = eolian, red = fluvial mudstone, bracket = measured section. The measured section for this study is annotated by a black bracket. Coloured bars represent approximate position of facies in outcrop, without reference to dips. Length of McCoy Brook Formation along the cliff face is ~ 200 m.



Figure 6.2 Prosauropods in the paleoenvironment of Wasson Bluff including the lake, dune field and basaltic paleo-cliff. Painting by Judi Pennanen (Atlantic Geoscience Society, 2001).

6.2 Taphonomy

The prosauropods were preserved within fluvial strata in a concentrated area (Fig. 2.2) but the cause of death has not been constrained. It is possible that they died in different areas of the fluvial channel and were concentrated together by the flow. Small trough cross-beds represent only a modest flow, which may not have had the strength to displace the dinosaur carcasses. However, a bloated carcass might float with very little water, allowing only a modest flow to concentrate the carcasses more readily.

Another possible scenario is a flooding event that may have overwhelmed the dinosaurs causing them to die and be buried quickly. The facies associations imply episodic flow, which could have been in the form of large flooding events and would support this hypothesis. Geometry of the basin also supports this scenario. At the time of preservation, the basin may have been fairly narrow inferred by a present day width of ~ 450 m (Olsen et al, 1989) allowing flooding events to be disastrous to animals that may have wandered into the narrow space in search of a water. An issue with this scenario is again, whether there was enough water and strong enough flow to overwhelm these prosauropods.

Due to the aridity of the hot-house climate of the Early Jurassic, another scenario might be a dried up water source. Water, which would have originally attracted these animals to the area, dried up (supported by desiccation cracks) and with no water or food the dinosaurs would not have been able to survive. Bones have not been found in eolian beds (which would be expected if the water had dried up) at the Princeton Quarry, which provides evidence against this scenario.

As the water was drying up the dinosaurs may have become entrapped in the still water-saturated sediment. Unable to escape, they would have been quickly preserved. This preservation style has been observed in China where small theropod dinosaurs were trapped in pits that are 1-2 m deep (Eberth et al, 2010). Localized areas of liquefaction were produced by large dinosaurs traveling across saturated sediments (Fig. 6.3) which then trapped smaller dinosaurs, producing soft sediment deformation and excellent preservation (Eberth et al, 2010). At Wasson Bluff, beds are thin and fairly continuous with no evidence of water escape structures associated with this preservation style. Due to their size, Princeton Quarry prosauropods were more likely to have produced localized liquefaction pits rather than falling victim to them.

A final scenario may be that these prosauropods entered the narrow basin and became overwhelmed by dense gases, possibly rising along faults, linked to the volcanic setting of the North Mountain Basalt. This type of scenario has been known to kill people and live stock during limnic eruptions. Limnic eruptions, which are eruptions from deep-water lakes, produce a sudden, large amount of dense carbon dioxide that can travel down hill and can kill by asphyxiation as it displaces oxygen and other gases.

A number of scenarios (Table 6.1) are possible for the ultimate demise of these prosauropods and possibly a combination of these scenarios. A combination of flooding overwhelming the dinosaurs in a narrow basin and then being concentrated by flow provides the most reasonable explanation with the little taphonomic evidence presented currently. Further constraints for the taphonomy will rely on future examination of the specimens themselves. Distribution, orientation, death postures and evidence of predation are all important factors that will contribute to the taphonomy.

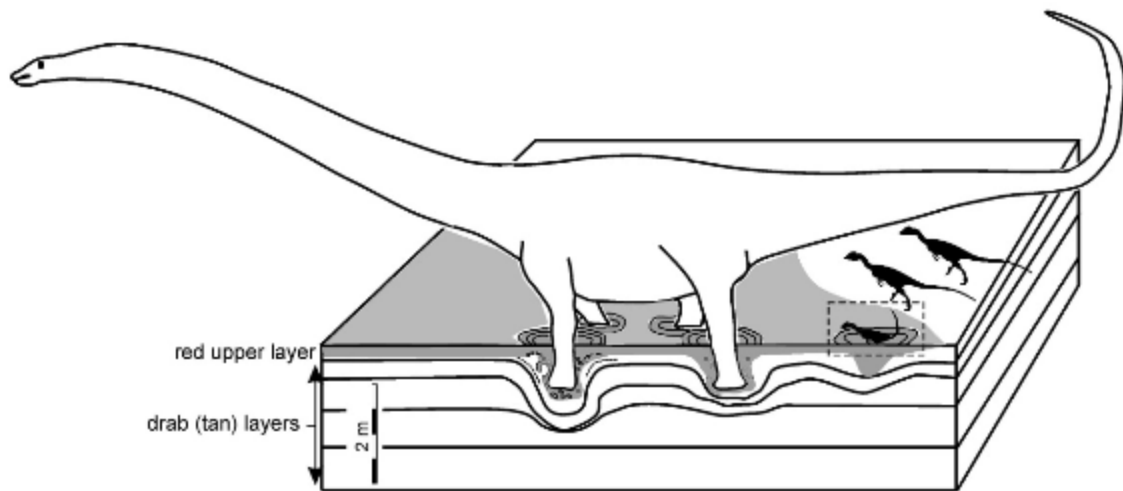


Figure 6.3 Large sauropod dinosaur producing localized pits where small theropods become entombed. Figure from Eberth et al. (2010).

Table 6.1 Summary of possible taphonomic scenarios for entombment of dinosaurs at Wasson Bluff.

Scenario	Supporting Evidence	Opposing Evidence
(1) concentrated by flow	bloated carcasses could float with little water	cross-beds represent only modest flow
(2) overwhelmed by flooding & narrow basin	episodic drainage, basin geometry	sedimentary structures suggest modest flow, water depth is undetermined
(3) dried up river	desiccation cracks	dinosaur preservation would also be in eolian dunes rather than just fluvial
(4) entrapped in soft sediment	concentrated preservation	no current evidence supporting water escape structures
(5) overwhelmed by gases	presence of North Mountain Basalt, basin geometry	currently no direct evidence to support this

6.3 Analogues

6.3.1 Barun Goyot Formation, Mongolia

The following lithological and specimen descriptions are based on Gradzinski and Jerzykiewicz (1974) who were geologists on expeditions to the Barun Goyot area in 1964, 1965, 1970 and 1971. The Upper Cretaceous Barun Goyot Formation is a red-bed sandstone unit containing eolian transverse dunes and water-deposited interdune sediments where dinosaur and mammal fossils have been excavated since 1922. This formation is located in the Northern Gobi Desert in the Mongolian People's Republic and provides a possible analogue for the Princeton Quarry (Olsen et al, 2005) at Wasson Bluff.

In this part of Mongolia, the Nemegt Basin, a graben flanked by Paleozoic horsts, is filled by the sedimentary Barun Goyot Formation and Nemegt Formation. The older Barun Goyot Formation has been interpreted as eolian dune deposits based on the presence of mega cross-stratified sandstone and lacustrine and fluvial deposits laid down in intermittent lakes and streams in the interdunal area, whereas the younger, Nemegt Formation is characterized by fluvial deposits.

The Barun Goyot Formation can be divided into five depositional types based on sedimentary structure and lithology 1) mega cross-stratified sandstones, 2) alternate claystones and sandstones, 3) diversely stratified sandstones, 4) structureless sandstones and 5) flat-bedded sandstones. Depositional type 1 is an eolian deposition whereas types 2-4 are fluvial and lacustrine.

The mega cross-stratified sandstones are laterally continuous beds composed of fine- or medium-grained sandstone that is moderately sorted. These beds range from 3 to

10 m thick, with smooth and horizontal contact surfaces. These mega cross-stratified sandstones interfinger with sandy claystone beds in some units. This interfingering suggests that waterlaid sandy claystone was deposited synchronously with eolian beds, probably in intermittent lakes that formed in interdunal areas.

At Wasson Bluff eolian cross-beds range from 0.6 to 2 m thick and are composed of fine- to medium-grained sandstone that is poorly to moderately sorted. Cross-set contacts are abrupt and linear, with the only evidence of interfingered eolian and mudstone beds being in FA3. Other evidence of an interfingering relationship may be present in other areas of the McCoy Brook Formation but appear scarce here because of the small section of Wasson Bluff studied.

All of the dinosaur and mammal remains within the Barun Goyot Formation are found within structureless sandstone (4) and small vertebrates are found within the diversified (3) or structure-less (4) sandstones. An ankylosaurid specimen was found in structure-less sandstone that passed laterally into typical deposits of a mega cross-stratified unit. One specimen was found within a mega cross-stratified sandstone but was not excavated due to the poor preservation quality.

At Wasson Bluff prosauropod specimens to date have been found within fluvial sediments, based on the interpretations of Olsen (2005) and the present, more detailed study. Specimens may exist in eolian deposits but, like some in the Barun Formation, may be poorly preserved. Overall, this Mongolian example is a good parallel to Wasson Bluff although Wasson Bluff appears to have only fluvial drainage systems with no evidence of intermittent lakes.

6.3.2 Kayenta and Navajo Formations, Northern Arizona

The following analogue is based on Middleton and Blakey (1983) for lithological description and Sertich and Loewen (2010) for description and preservation of basal sauropodomorphs. The Jurassic Kayenta and Navajo Formations are the two youngest formations of the Glen Canyon Group, located in northern Arizona and southern Utah, characterized by formations of eolian and fluvial sandstones with preservation of basal sauropodomorph remains. Sandstones deposited within the eolian systems are characterized by large-scale cross-bedded sandstones that are fine- to medium- grained, moderately well sorted and with well-rounded grains. Most of these sandstones are extremely quartz rich. A majority of the Navajo sandstone was deposited with these characteristics. The Kayenta fluvial strata were deposited by braided and meandering channel systems, with vertically accreted floodplains and small lacustrine buildups. These deposits are lenticular whereas eolian deposits are tabular. The fluvial sandstones are poorly sorted, have more silt and clay matrix than eolian sandstones and have grains that range from sub-angular to sub-rounded. Fluvial strata are also characterized by abundant lithic grains. Carbonate and chert are present in both eolian and fluvial deposits.

The fluvial Kayenta Formation comprises reddish brown sandstone interbedded with subordinate amounts of gray to red mudstone. The strata have channel bases, cross stratification with sets that range from ~20 – 40 cm thick, horizontal stratification, and grade laterally into reddish brown siltstone and claystone with minor sandstone. This formation was interpreted as a sandy braided and meandering fluvial system.

The Navajo Formation is of eolian origin with large complex dunes and broad interdunal areas. In interdunal areas with ponds, fresh water carbonate accumulated.

These formations represent a shift from a largely fluvial system to an eolian dominated system. In southern Utah and northeastern Arizona, these formations intertongue.

A basal sauropodomorph, *Seitaad* (UMNH VP 18040) (Fig. 6.4), which is closely related to plateosaurid or massospondylid 'prosauropod' reptiles (Sertich and Loewen, 2010), is preserved within a massive, Navajo Formation sandstone bed that is in contact with the Kayenta Formation and represents a switch in depositional environment. The bed that this prosauropod is preserved in does not have eolian structures but is petrologically equivalent to eolian sandstones that display dune sets and dune slumps, implying that it too, is eolian. The bed has been understood to be a local dune collapse which preserved the dinosaur (Sertich and Loewen, 2010). Three other basal sauropodomorphs (Fig. 6.4) have been collected and documented in the Glen Canyon Group, one of which is an indeterminate taxon due to the fragmented remains (MNA 7233) and another (UCMP 82961) belongs to Plateosauria (Middleton and Blakey, 1983).

This analogue represents a large-scale version of Wasson Bluff. At Wasson Bluff the strata that crops out only allows observation of small section of the basin fill, whereas the Navajo and Kayenta formations crop out in large sections. The Kayenta-Navajo interaction also depicts a shift in depositional environments whereas Wasson Bluff is an eolian-dominated environment with drainage areas interacting with eolian dunes.

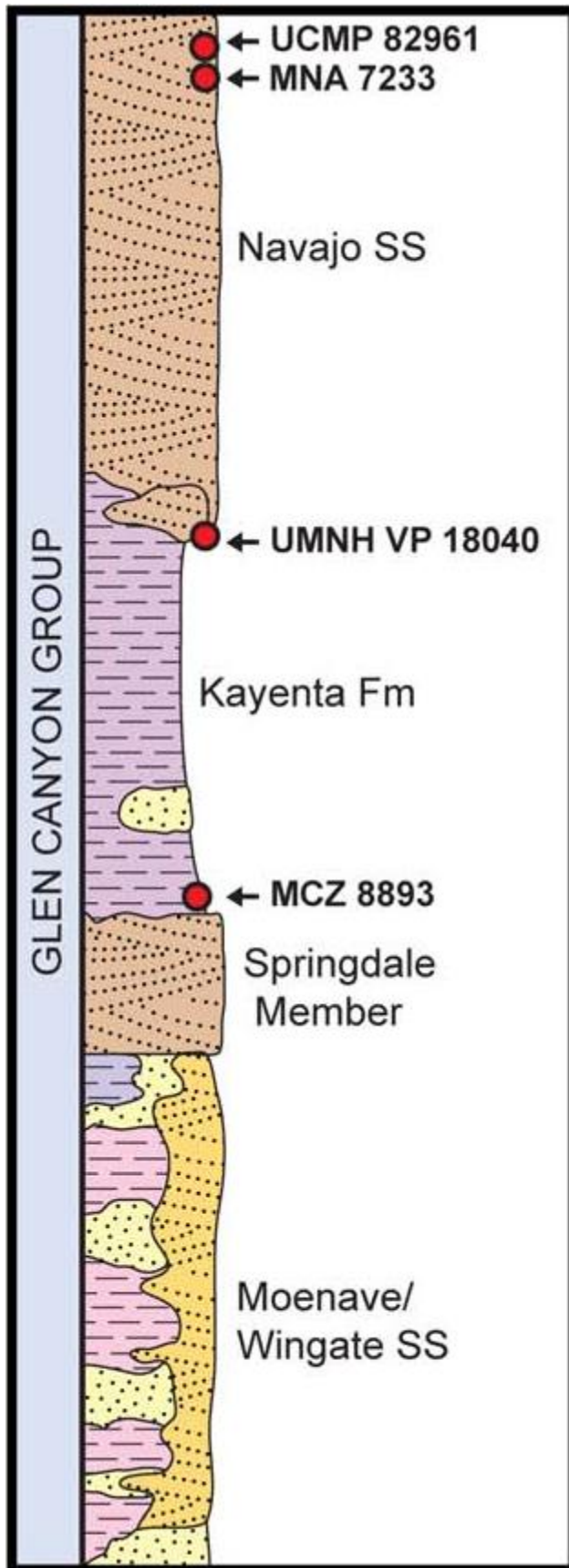


Figure 6.4 Stratigraphic column from Sertich and Loewen (2010) of the Lower Jurassic Glen Canyon Group showing the location of sauropodomorph specimens found in the Kayenta and Navajo Formations.

6.3.3 Modern Analogue

A modern analogue for Wasson Bluff is the dune fields in western Mongolia where lakes and fluvial systems persist throughout the desert climate. In this environment dunes appear to migrate over fluvial systems and look as if they are able to dictate fluvial drainage (Fig 6.5). When this arid area gets precipitation, braided fluvial systems are likely able to reestablish themselves. At Wasson Bluff the dune field would have been infilling a micro-basin and high precipitation events may have caused a smaller scale braided river system similar to western Mongolia's or flooding events that were constrained by basin borders. The fluvial strata cropping out at Wasson Bluff provide little information on channel dimensions presently.



Figure 6.5 Modern fluvial and eolian interaction in the dune fields of Western Mongolia to the south of Zavkhan. Photo from Google Earth, 2014.

6.4 Future Work

Future work for the McCoy Brook Formation at Wasson Bluff could include more detailed stratigraphic analysis of the entire basin fill. A high-resolution stratigraphic column for the entire section may lend itself to highlighting high-potential area for future excavation sites. Along with the sedimentology of the basin, the structure could be analyzed at a higher resolution. Sedimentology and structure go hand-in-hand in this area, and it is difficult to correlate beds without structural analysis in these highly faulted cliff sections. At the Princeton Quarry site, beach debris could be cleared away to analyze strata directly beneath the bone bed. This sedimentological information would be useful in constraining taphonomic scenarios. Strata should also be monitored frequently as the world's highest tides will continue to reveal new outcrop.

A detailed provenance study could be useful for the area. Fission-track dating on zircon inclusions within quartz grains would provide ages of potential source areas. Zircons remain at a stable phase during sedimentation (Morton and Hallsworth, 1999), making them useful for a provenance study. A heavy mineral analysis may also be beneficial to a provenance study, as factors that control heavy mineral assemblages are fairly well known. Scanning electron microscope photos of quartz grains, used to analyze pitting surfaces or lack thereof would provide more evidence for the separation of eolian and fluvial deposition.

Taphonomic terms are based on Rogers (1994). As mentioned earlier, future taphonomic analysis will rely on analysis of the bones themselves. Many features to determine taphonomy have been already been documented including number of individuals, sample size, state of articulation and association and distortion due to faulting.

Using the bone map, and specimens collected during previous digs, further details such as orientation, distribution and surface modifications can be studied and used in conjunction with data already collected. After a complete study of the bones, along with the stratigraphic column produced in this study, a nearly complete taphonomic history of the Princeton Quarry can be reconstructed.

Chapter 7: Conclusions

Early Jurassic strata at Wasson Bluff, represent an eolian dune field, which infilled a half-graben formed on the surface of the North Mountain Basalt. At the Princeton Quarry, fluvial drainage, implied by ripples, desiccation cracks and trough-cross bedding, ran through this dune field on an episodic basis. Within these drainage areas prosauropod skeletal remains have been preserved due to rapid burial.

The Cobequid Highlands to the north of the basin are the most probable source of sediment infill as petrography implies a proximal metamorphic, igneous and sedimentary source. Grain size analysis with supporting petrographic analysis establish three facies present at the Princeton Quarry: red-brown mudstone, orange brown sandstone and grey-brown sandstone. Two facies associations lead to the interpretation of fluvial (FA 1) and eolian (FA 2) depositional environments.

Regular gypsum nodules throughout fluvial and eolian strata at Wasson Bluff suggest that this was an arid and hot paleoenvironment which is confirmed by the 26°N paleolatitude proposed by Kent and Tauxe (2005). As prosauropods have been discovered in fluvial sediment and animals living in this climate are likely to stay close to a water source, it is reasonable to suggest that discovery potential of new material may be higher within fluvial sediment. Canada's oldest dinosaurs may have been overwhelmed by flooding in a narrow basin and/or a moderate flow may have been able to concentrate the bloated carcasses. Future work on collected specimens will provide more taphonomic constraints.

Appendix A: Summary of lithological observation by bed.

Bed	Total Thickness (cm)	Bed Thickness (cm)	Contact (basal)	Facies	Sediment Type	Grain Size	phi	Grain Roundness	Sorting	Colour	Mica Abundance	Stratification and Sedimentary Structures	Gyps um nodul	Fossils	Notes
1	35 cm	35 cm	n/a	2	muddy sand	fine to medium sand	3-0 peak: 1.5	subrounded	very poorly sorted	orange brown	moderate mica	tough cross bedding, weakly stratified	Y	Prosauropod	Basalt boulders (30, 16cm), subequant boulders, scattered, <5% cobbles to boulders size. Main bone bed
2	44 cm	9 cm	abrupt	1	mud	fine to medium silt	7-4 peak: 6.5	n/a	poorly sorted	red brown	moderate mica	stratified	N	none	top contact: sand filled into mud cracks
3	51 cm	7 cm	abrupt	2	muddy sand	fine to medium sand	3-0 peak: 2	subrounded	very poorly sorted	orange brown	not noted	massive	Y	none	
4	70 cm	19 cm	abrupt	1	sandy mud	fine-medium silt to fine medium sand	3-0 and 7-5	n/a	very poorly sorted	red brown, grey-green mottles	moderate mica	laminations?, Unidirectional, Mud cracks on top surface,	N	none	basalt boulders present 40 cm on contact with LV3
5	89 cm	19 cm	abrupt, wavy	2	muddy sand	fine sand	3-0 peak: 2	sub-angular to sub-rounded	poorly sorted	orange brown	moderate mica	weak stratification, possible cross beds ~5cm	Y	none	gypsum nodules 1-2mm diameter
6	95 cm	6 cm	abrupt	2 1	muddy sand interbedded with mud drapes	fine sand	A: 3-1 peak: 2.8 B: 10-2	subrounded	poorly sorted	brown sand - orange brown	mica rich on laminae surfaces	sand - weakly stratified	Y in sand	none	3 mud drapes less than 0.5 cm thick each
7	113 cm	18 cm	abrupt	2	muddy sand	fine sand	0-4 peak: 2	sub-angular to sub-rounded	poorly sorted	orange brown	not noted	weakly stratified	Y	none	
8	117 cm	4 cm	abrupt	1	sandy mud	day to fine silt & fine sand	1-4 and 5-10	n/a	very poorly sorted	red	not noted	stratified	N	none	
9	124 cm	7 cm	abrupt	2 1	muddy sand interbedded with mud drapes	very fine to fine sand	1-7-4 peak: 2.5	no data	very poorly sorted	orange brown sand	mica rich on laminae surfaces	weakly stratified	N	none	3-4 drapes that 0.5 mm thick
10	142 cm	18 cm	abrupt	2	muddy sand	fine to medium sand	(neg)0.5-3.5; peak: 2.5	sub-angular	poorly sorted	orange brown	few mica	slightly diffuse concave up surfaces (interp: tough cross beds ~5cm thick)	Y	none	
11	184 cm	42 cm	abrupt	2	muddy sand	fine to medium sand	0-4 peak: 1.75	sub-angular	poorly sorted	orange brown	few mica	tough cross beds, weak stratification	Y	disarticulated prosauropod present	basalt boulders present
12	185 cm	1 cm	abrupt	1	mud	fine to medium silt	4-10 peak: 6.5	n/a	moderately sorted*	red brown	not noted	stratified, lamination	N	none	
13	189 cm	4 cm	abrupt	2	sand*	medium sand*	no data	no data	poorly sorted*	orange brown	few mica	not noted	Y	none	
14	190 cm	1 cm	abrupt	1	mud*	fine silt*	no data	n/a	moderately sorted*	red brown	not noted	stratified	N	none	
15	198 cm	8 cm	abrupt	2	sand*	medium sand*	no data	no data	poorly sorted*	orange brown	not noted	not noted	Y	none	
16	198.5 cm	0.5 cm	abrupt	1	mud*	fine silt*	no data	n/a	moderately sorted*	red brown	not noted	stratified	N	none	
17	204.5 cm	6 cm	abrupt	2	sand*	medium sand*	no data	no data	poorly sorted*	orange brown	not noted	not noted	Y	none	
18	205 cm	0.5 cm	abrupt	1	mud*	fine silt*	no data	n/a	moderately sorted*	red brown	not noted	stratified	N	none	
19	405 cm	200 cm	abrupt	3	sand	fine to medium sand	0-4 peak: 1.5	no data	poorly sorted	light grey brown	few mica	laminated (light and dark), tough cross beds, possible channel scour	Y	none	cross beds 11/48 SW, possible Channel scour trend: 243 (M4,P3B), Gypsum nodules 2.5 mm diameter
20	407 cm	2 cm	abrupt	1	mud*	fine silt*	no data	n/a	moderately sorted*	red brown	not noted	stratified	N	none	2 cm at bottom and thins left (fault?)
21	507 cm	100 cm	abrupt	3	sand	medium sand	0-4 peak: 1	sub-angular to sub-rounded	poorly sorted	light grey brown	qtz, fsp, matrics	cross beds, possible channel scour	Y	none	cross beds 284/52 SW (M5), Channel trend 230 (M7)
22	567 cm	60 cm	abrupt	3	sand	medium to coarse sand	0-2 peak: 1	no data	moderately sorted	light grey brown	qtz, fsp, matrics	laminated (light and dark), cross beds	Y	none	cross beds 274/50 S (M6)

* this data is from field observation and not from grain size analysis

Appendix B: Summary of grain size analysis by bed.

Bed	Sediment Type	Grain Size	Sorting	Mode	distribution (gravistat)	Distribution (PSS)	mean (phi)	SD (phi)	Skewness (phi)	Kurtosis (phi)	mean (phi)	SD (phi)	Skewness (phi)	Kurtosis (phi)	Kurtosis Description
							method of moments				folk & ward				
22	sand	medium sand	moderately well sorted	unimodal	sand: 97.2% mud: 2.8%	Sand:97.23% Silt:1.91% Clay:0.86% Mud:2.77%	1.365	1.139	4.504	28.39	1.177	0.594	0.312	1.59	very leptokurtic
21	sand	medium sand	poorly sorted	unimodal	sand: 92.8% mud: 7.2%	Sand: 92.77% Silt:5.13% Clay:2.10% Mud:7.23%	2.009	1.621	2.923	12.71	1.757	1.177	0.554	1.804	very leptokurtic
20	n/a	n/a	n/a	n/a	n/a	n/a	n/a	n/a	n/a	n/a	n/a	n/a	n/a	n/a	n/a
19	sand	medium sand	poorly sorted	unimodal	sand: 90.9% mud: 9.1%	Sand:90.91% Silt:6.50% Clay:2.59% Mud:9.09%	2.398	1.668	2.691	11.1	2.109	1.259	0.461	1.976	very leptokurtic
18	n/a	n/a	n/a	n/a	n/a	n/a	n/a	n/a	n/a	n/a	n/a	n/a	n/a	n/a	n/a
17	n/a	n/a	n/a	n/a	n/a	n/a	n/a	n/a	n/a	n/a	n/a	n/a	n/a	n/a	n/a
16	n/a	n/a	n/a	n/a	n/a	n/a	n/a	n/a	n/a	n/a	n/a	n/a	n/a	n/a	n/a
15	n/a	n/a	n/a	n/a	n/a	n/a	n/a	n/a	n/a	n/a	n/a	n/a	n/a	n/a	n/a
14	n/a	n/a	n/a	n/a	n/a	n/a	n/a	n/a	n/a	n/a	n/a	n/a	n/a	n/a	n/a
13	n/a	n/a	n/a	n/a	n/a	n/a	n/a	n/a	n/a	n/a	n/a	n/a	n/a	n/a	n/a
12	mud	medium silt	poorly sorted	unimodal	mud: 100%	Sand:0% Silt:67.64% Clay:32.36 Mud:100%	7.454	1.452	0.42	2.592	7.435	1.49	0.18	0.989	mesokurtic
11	muddy sand	very coarse silt fine sand	poorly sorted	unimodal	sand: 82% mud: 18%	Sand:81.96% Silt:12.71% Clay:5.33% Mud:18.04%	2.93	2.166	1.739	5.497	2.706	1.91	0.5	1.897	very leptokurtic
10	muddy sand	very coarse silty fine sand	poorly sorted	unimodal	sand: 84.8% mud: 15.2%	Sand: 84.81% Silt:11.35% Clay:3.84% Mud:15.19%	2.937	1.906	1.841	6.686	2.633	1.603	0.297	2.123	very leptokurtic
8	sandy mud	fine sandy fine silt	very poorly sorted	bimodal	sand: 25.1% mud: 74.9%	Sand:25.09% Silt:41.54% Clay:33.36% Mud:74.91%	6.499	2.629	-0.243	1.899	6.441	2.793	-0.207	0.73	platykurtic
7	muddy sand	medium silty fine sand	poorly sorted	unimodal	sand: 84.4% mud:15.6%	Sand: 84.41% Silt:11.22% Clay:4.37% Mud:15.59%	2.983	1.955	1.915	6.522	2.66	1.605	0.399	2.18	very leptokurtic
6B	B: sandy mud	very fine sandy very coarse silt	very poorly sorted	trimodal	sand: 38.4% mud: 61.6%	sand:38.40% Silt:40.97% Clay:20.64% Mud:61.6%	5.56	2.496	0.452	1.961	5.494	2.535	0.282	0.718	platykurtic
6A	A: muddy sand	A: medium silty fine sand	poorly sorted	unimodal	sand: 82.1% mud: 17.9%	Sand: 81.51% Silt:13.04% Clay:5.44% Mud:18.49%	3.067	2.042	1.822	5.875	2.879	1.747	0.545	2.436	very leptokurtic
5	muddy sand	very coarse silty fine sand	poorly sorted	unimodal	sand: 85.9% mud: 14.1%	Sand:85.91% Silt:10.23% Clay:3.86% Mud:14.09%	2.866	1.893	1.993	7.062	2.529	1.537	0.352	2.118	very leptokurtic
4	sandy mud	medium sandy medium silt	very poorly sorted	bimodal	sand: 32.8% mud: 67.2%	Sand:32.80% Silt:43.55% Clay:23.65% Mud:67.2%	5.629	2.94	-0.189	1.801	5.583	3.055	-0.222	0.68	platykurtic
3	muddy sand	fine silt fine sand	very poorly sorted	unimodal	sand: 80% mud: 20%	Sand: 79.97% Silt:13.13% Clay:6.90% Mud:20.03%	3.131	2.332	1.59	4.523	3.224	2.262	0.628	2.118	very leptokurtic
2	mud	medium silt	poorly sorted	unimodal	mud: 100%	Sand: 0% Silt:71.97% Clay:28.03% Mud:100%	7.309	1.401	0.535	2.81	7.272	1.421	0.201	1.027	mesokurtic
1	muddy sand	medium silt medium sand	very poorly sorted	unimodal	sand: 81.3% mud: 18.7%	Sand: 81.29% Silt: 13.28% Clay: 5.43 Mud:18.71	2.845	2.246	1.661	5.02	2.686	2.024	0.567	1.804	very leptokurtic
east crossbeds	sand	medium sand	moderately sorted	unimodal	sand: 95.2% mud: 4.8%	Sand: 95.07% Silt:3.40% Clay:1.53% Mud:4.93%	1.697	1.405	3.552	18.05	1.472	0.832	0.367	1.488	leptokurtic

References

- Atlantic Geoscience Society, 2001.** The Last Billion Years: A Geological History of the Maritime Provinces of Canada. Halifax: Atlantic Geoscience Society, Nimbus Publishing.
- Beckman Coulter Inc., 2011.** LS 13 320 Laser Diffraction Particle Analyzer, Instructions for Use.
- Blackburn, T. J., Olsen P.E., Bowring, S. A., McLean, N. M., Kent, D. V., Puffer, J., McHone, G., Rasbury, E.T., and Et-Touhami, M. 2013.** Zircon U-Pb Geochronology Links the End-Triassic Extinction with the Central Atlantic Magmatic Province. *Science* 340, p. 941-945.
- Blott, S. J. and Pye, K. 2001.** GRADISTAT: a grain size distribution and statistics package for the analysis of unconsolidated sediments. *Earth Surface Processes and Landforms* 26, P. 1237-1248.
- Cirilli, S., Marzoli, A., Tanner, L., Bertrand, H., Buratti, N., Jourdan, F., Bellieni, G., Kontak, D. and Renne, P.R. 2009.** Latest Triassic onset of the Central Atlantic Magmatic Province (CAMP) volcanism in the Fundy Basin (Nova Scotia): New stratigraphic constraints. *Earth and Planetary Science Letters* 286, p. 514-525.
- Eberth, D. A., Xing, X. and Clark, J. M. 2010.** Dinosaur death pits from the Jurassic of China. *Palaios* 25, p.112-125.
- Fedak, T. J. 2006.** Description and Evolutionary Significance of the Sauropodomorph Dinosaurs from the Early Jurassic (Hettangian) McCoy Brook Formation. Ph. D. thesis, Dalhousie University, Halifax, N.S.
- Frakes, L.A. 1979.** Climate Throughout Geologic Time. Elsevier Scientific Publishing Company, New York, N.Y.
- Friedman, G. M. 1961.** Distinction between dune, beach, and river sands from their textural characteristics. *Journal of Sedimentary Petrology* 31, p.514-529.
- Folk, R.L. 1971.** Longitudinal dunes of the northwestern edge of the Simpson Desert, Northern Territory, Australia, 1. Geomorphology and grain size relationships. *Sedimentology* 16, p.5-54.
- Folk, R. L. 1974.** Petrology of Sedimentary Rocks. Austin Texas, Hemphill, 182.
- Fowell, S.J., and Olsen, P.E. 1993.** Time calibration of Triassic-Jurassic microfloral turnover, eastern North America. *Tectonophysics* 222, p. 361-369.

- Gradzinski, R. and Jerzykiewicz, T. 1974.** Dinosaur- and mammal bearing Aeolian and associated deposits of the Upper Cretaceous in the Gobi Desert (Mongolia). *Sedimentary Geology* 12, p. 249-278.
- Hubert, J. F. and Mertz, K. A. 1984.** Eolian sandstones in Upper Triassic-Lower Jurassic Red Beds of the Fundy Basin, Nova Scotia. *Journal of Sedimentary Petrology* 54, p.798-810.
- Kent, D. V. and Olsen, P. E. 2000.** Magnetic polarity stratigraphy and paleolatitude of the Triassic-Jurassic Blomidon Formation in the Fundy Rift basin (Canada): impacts for early Mesozoic tropical climate gradients. *Earth and Planetary Science Letters* 179, p. 311-324.
- Kent, D.V. and Tauxe, L. 2005.** Corrected Late Triassic Latitudes for Continents Adjacent to the North Atlantic. *Science* 307, 240-244.
- Langford, R.P. 1989.** Fluvial-aeolian interactions: Part I, modern systems. *Sedimentology* 36 p. 1023-1035.
- Malvern Instruments, www.malvern.com.** Retrieved March 3, 2014, from <http://www.malvern.com/en/products/measurement-type/particle-size>
- Middleton, L.T. and Blakey, R.C. 1983.** Processes and Controls on the intertonguing of the Kayenta and Navajo Formations, Northern Arizona: eolian-fluvial interactions. *In* *Eolian Sediments and Processes* (Ed. By M.E. Brookfield and T.S. Ahlbrandt). Dev. Sediment, Elsevier, Amsterdam.38, 613-634.
- Morton, A. C. and Hallsworth, C. R. 1999.** Processes controlling the composition of heavy mineral assemblages in sandstones. *Sedimentary Geology*, 124 p. 3-29.
- Olsen, P.E. 1988.** Paleontology and paleoecology of the Newark Supergroup (early Mesozoic, eastern North America). Chapter 8 *in* *Paleoecology and Paleoenvironment of the Continental Early Mesozoic Newark Supergroup of Eastern North America* *In* Manspeizer, W. (ed), *Triassic-Jurassic Rifting and the Opening of the Atlantic Ocean*, Elsevier, Amsterdam, p.185-230.
- Olsen, P. E., Koeberl, C., Huber, H., Montanari, A., Fowell, S. J., Et-Touhami, M., and Kent, D. V. 2012.** Continental Triassic-Jurassic boundary in central Pangea: Recent progress and discussion of an Ir anomaly. *The Geological Society of America, Special Paper*, 356 p. 505-522.
- Olsen, P.E., Schlische, R.W., and Gore, P.J.W. 1989.** Field Guide to the Tectonics, stratigraphy, sedimentology, and paleontology of the Newark Supergroup, eastern North America: *International Geological Congress Guidebooks for Field Trips T351*, 174 p. 149-161.
- Olsen, P. E., Whiteside, J. H. and Fedak, T. J. 2005.** Field Trip A7: Triassic-Jurassic faunal and floral transition in the Fundy Basin, Nova Scotia. *Geological Association of Canada*,

Mineralogical Association of Canada, Canadian Society of Petroleum Geologists, Canadian Society of Soil Sciences Joint Meeting, Halifax, May 2005, AGS Special Publication Number 26.

Price, C., Gibling, M., Fedak, T. 2014. Lithofacies of the Early Jurassic vertebrate-bearing Scots Bay Member at Wsson Bluff, Nova Scotia. Atlantic Geoscience Society Annual Conference, Wolfville, NS, February 7-9.

Rogers 1994. Collecting taphonomic data from vertebrate localities. Chapter 3 *in* Vertebrate Paleontological Techniques 1 (Ed. By P. Leiggi and P. May), Cambridge University Press. p. 47-57.

Scotese, C. R. 2001. Atlas of Earth History, Volume 1, Paleogeography, PALEOMAP Project, Arlington, Texas, p. 52.

Sereno, P.C. 1997. The origin and Evolution of dinosaurs. Annual Review of Earth and Planetary Sciences 25, p. 435-489.

Sereno, P.C. 1986. Phylogeny of the bird-hipped dinosaurs (order Ornithischia). National Geographic 2 p. 234-256.

Sertich, J. J. W. and Loewen, M. A. 2010. A New Basal Sauropodomorph Dinosaur from the Lower Jurassic Navajo Sandstone of Southern Utah. PLoS ONE 5 (3), p. 1-17.

Tanner, L. H. and Hubert, J. F. 1991. Basalt Breccias and Conglomerates in the Lower Jurassic McCoy Brook Formation, Fundy Basin, Nova Scotia: Differentiation of talus and debris-flow deposits. Journal of Sedimentary Petrology 61, p. 15-27.

Tanner, L. H. 1996. Formal definition of the Lower McCoy Brook Formation, Fundy Rift Basin, eastern Canada. Atlantic Geology 32, p. 127-135.

Yates, A. M., Bonnan, M. F., Neveling, J., Chinsamy, A. and Blackbeard, M. G. 2009. A new transitional sauropodomorph dinosaur from the Early Jurassic of South Africa and the evolution of sauropod feeding and quadrupedalism. Proceedings of the Royal Society of London B 277: 787-794.

Zervas, D., Nichols, G. J., Hall, R., Smyth, H. R., Luthje, C. and Murtagh, F. 2009. Sedlog: A shareware program for drawing graphic logs and log data manipulation. Computers & Geosciences, 35 (10) p. 2151-2159.